

# New insights into solubility control mechanisms and the role of particle- and colloid-facilitated transport of metals in contaminated soils

Åsa Löv

*Faculty of Natural Resources and Agricultural Sciences  
Department of Soil and Environment  
Uppsala*

Doctoral thesis  
Swedish University of Agricultural Sciences  
Uppsala 2018

Acta Universitatis agriculturae Sueciae

2018:56

ISSN 1652-6880

ISBN (print version) 978-91-7760-252-1

ISBN (electronic version) 978-91-7760-253-8

© 2018 Åsa Löv, Uppsala

Print: SLU Service/Repro, Uppsala 2018

# New insights into solubility control mechanisms and the role of particle- and colloid-facilitated transport of metals in contaminated soils

## Abstract

Particle- and colloid-mediated transport of metals can be an important leaching pathway in contaminated soils, making it necessary to include this process in risk assessments of contaminant transport. In this thesis, mechanisms involved in transport of particulate, colloidal and truly dissolved lead, chromium, zinc, arsenic and antimony were studied in an irrigation experiment performed on intact soil columns from four historically contaminated soils. Speciation of lead and chromium in bulk soil, particles and colloids was studied using extended X-ray absorption fine structure (EXAFS) spectroscopy and geochemical modelling. The ability of three standardised leaching tests (a percolation test and two batch tests using deionised water or calcium chloride) to describe leaching from intact soil columns was also investigated, using size-based elemental fractionation.

The results from the irrigation experiment suggested that the tendency for metal(loid)s to be transported with particles and colloids followed the order: lead > chromium > zinc > arsenic > antimony. There were large differences between the soils as regards particulate and colloidal leaching of lead and chromium, whereas the differences between irrigation intensities were minor. Thus, particle- and colloid-mediated metal transport was mainly governed by soil properties. Interactions between lead and iron in particles and colloids were confirmed by EXAFS and geochemical modelling. In contrast, lead in bulk soil was mainly bound to organic matter in two soils and to aluminium hydroxide in one soil. In one soil, lead probably occurred mainly as mimetite ( $\text{Pb}_5(\text{AsO}_4)_3\text{Cl}$ ) in the bulk soil and in the particulate and colloidal phases. Using EXAFS and geochemical modelling, chromium in particles and colloids, and in the bulk soil, was identified as a dimeric chromium(III) complex with organic matter.

A percolation test at a liquid-to-solid ratio of 10 proved useful for conservatively categorising soils into high-risk soils with respect to mobilisation of particulate and colloidal metal(loid)s. In batch tests, using calcium chloride instead of deionised water enabled better prediction of the truly dissolved fraction for elements prone to colloidal mobilisation, such as lead.

These novel findings can be used to improve the description of transport processes in risk assessments, resulting in more accurate evaluations of total metal transport and metal solubility in historically contaminated soils.

*Keywords:* Contaminated soil, intact soil columns, irrigation experiment, particles, colloids, metal(loid)s, lead, chromium, EXAFS, geochemical modelling, leaching tests  
*Author's address:* Åsa Löv, SLU, Department of Soil and Environment, P.O. Box 7014, 750 07 Uppsala, Sweden.

# Dedication

To science.

# Contents

<b>List of publications</b>	<b>7</b>
<b>Abbreviations</b>	<b>9</b>
<b>1 Introduction</b>	<b>11</b>
<b>2 Rationale of thesis</b>	<b>13</b>
<b>3 Aim</b>	<b>15</b>
<b>4 Structure of thesis</b>	<b>17</b>
<b>5 Methods</b>	<b>19</b>
5.1 Study sites and sampling of intact soil columns	19
5.2 Irrigation experiment	20
5.3 Soil physical characterisation	21
5.4 Size-based fractionation of elements	21
5.5 EXAFS	22
5.6 Time- and pH-dependent solubility	23
5.7 Geochemical modelling	23
5.8 Standardised leaching tests	24
<b>6 Bulk soil properties</b>	<b>25</b>
6.1 Chemical properties of experimental soils (Paper I-IV)	25
6.2 Hydraulic properties of experimental soils (Papers II and III)	27
<b>7 Metal solubility and speciation in bulk soil</b>	<b>29</b>
7.1 Time-dependent solubility at ambient pH of lead, chromium, zinc, arsenic and antimony (Papers I and III-IV)	30
7.2 Solubility and speciation of lead (Paper I)	31
7.3 Solubility and speciation of chromium (Paper III)	33

<b>8</b>	<b>Particle- and colloid facilitated transport of metals</b>	<b>37</b>
8.1	Partitioning of iron, aluminium, manganese and organic carbon (Papers II-IV)	38
8.1.1	Speciation of iron in bulk soil, particles and colloids (Papers II and III)	39
8.2	Partitioning of lead, chromium, zinc, arsenic and antimony (Paper II-IV)	41
8.2.1	Speciation of lead in particles and colloids (Paper II)	42
8.2.2	Speciation of chromium in particles and colloids (Paper III)	45
8.3	Effect of irrigation intensity on transport of lead and chromium	46
8.3.1	Effect of irrigation intensity on transport of lead (Paper II)	46
8.3.2	Effect of irrigation intensity on transport of chromium (Paper III)	48
<b>9</b>	<b>Mechanisms controlling transport of lead and chromium in soils</b>	<b>51</b>
9.1	Soil factors controlling leaching of particulate and colloidal lead (Paper II)	51
9.2	Conceptual model of lead and chromium leaching in non-macroporous soils	52
<b>10</b>	<b>Evaluation of three standardised leaching tests (Paper IV)</b>	<b>55</b>
10.1	Evaluation of contact time	56
10.2	Percolation experiment (CEN/TS 14405)	57
10.3	Batch test with deionised water (EN 12457-2)	59
10.4	Batch test with 1 mM CaCl <sub>2</sub> (ISO/TS 21268-2)	60
10.5	Which leaching test is preferred and why?	61
<b>11</b>	<b>Conclusions</b>	<b>63</b>
<b>12</b>	<b>Environmental implications and future risk assessments</b>	<b>65</b>
12.1	Approach for future risk assessments	66
12.1.1	'Transport K <sub>d</sub> ' for non-macroporous soils	66
12.1.2	Geochemical modelling in risk assessments	68
	<b>References</b>	<b>69</b>
	<b>Acknowledgements</b>	<b>77</b>

## List of publications

This thesis is based on the work contained in the following papers, referred to by Roman numerals in the text:

- I. Sjöstedt, C., Löv, Å., Olivecrona, Z., Boye, K. & Kleja, D.B. (2018). Improved geochemical modeling of lead solubility in contaminated soils by considering colloidal fractions and solid phase EXAFS speciation. *Applied Geochemistry* 92, 110-120.  
DOI: 10.1016/j.apgeochem.2018.01.014
- II. Löv, Å., Cornelis, G., Larsbo, M., Persson, I., Sjöstedt, C., Gustafsson, J.P., Boye, K. & Kleja, D.B. (2018). Particle and colloid facilitated Pb transport in four historically contaminated soils – Speciation and effect of irrigation intensity. *Applied Geochemistry* 96, 327-338.  
DOI: 10.1016/j.apgeochem.2018.07.012
- III. Löv, Å., Sjöstedt, C., Larsbo, M., Persson, I., Gustafsson, J.P., Cornelis, G. & Kleja, D.B. (2017). Solubility and transport of Cr(III) in a historically contaminated soil – Evidence of a rapidly reacting dimeric Cr(III) organic matter complex. *Chemosphere* 189, 709-716.  
DOI: 10.1016/j.chemosphere.2017.09.088
- IV. Löv, Å., Larsbo, M., Sjöstedt, C., Cornelis, G., Gustafsson, J.P. & Kleja, D.B. Evaluation of the ability of three standardised leaching tests to predict leaching of Pb, Zn, As and Sb from intact soil columns using size-based elemental fractionation.  
*Submitted manuscript.*

Papers I-III are reproduced with the permission of the publishers.

The contribution of Åsa Löv to the papers included in this thesis was as follows:

- I. Planned the study together with the co-authors. Assisted in the laboratory work, data analysis and writing
- II. Planned the study together with the co-authors. Performed the laboratory work, EXAFS analysis, geochemical modelling and writing, with assistance from the co-authors.
- III. Planned the study together with the co-authors. Performed the laboratory work, EXAFS analysis, geochemical modelling and writing, with assistance from the co-authors.
- IV. Planned the study together with the last author. Performed the irrigation experiment, data analysis and writing, with assistance from the co-authors.

## Abbreviations

Å	Ångström
BTC	Breakthrough curve
CD-MUSIC	Charge distribution multisite complexation
CN	Coordination number
DOC	Dissolved organic carbon
DOM	Dissolved organic matter
EPA	Environmental protection agency
EXAFS	Extended x-ray absorption fine structure
FA	Fulvic acid
HA	Humic acid
kDa	Kilo Dalton
L/S	Liquid-to-solid ratio
OC	Organic carbon
PPHA	Pahokee peat humic acid
PV <sub>eff</sub>	Effective pore volume
SMHI	Swedish Meteorological and Hydrological Institute
SOM	Soil organic matter
TOC	Total organic carbon
XRT	X-ray tomography



# 1 Introduction

In Sweden today there are about 85 000 potentially contaminated sites, 7000 of which are rated as high risk areas and 1000 as very high risk areas to human health or to the environment (Swedish EPA, 2018). Remediation of contaminated sites is a costly activity and a thorough risk assessment should be performed before a decision is made regarding remediation. Understanding the nature of the leaching mechanisms of contaminants in soil is essential for estimating the magnitude of potential transport of contaminants.

In the Swedish model for risk assessments, which is similar to the Dutch and US models, protection targets such as groundwater, surface water, soil ecosystem and humans are identified. In standard risk assessments today, the solubility, and thereby transport, of an element is described as an equilibrium partition process between solid and solution phases. Hence, the potential transport of elements with particles and colloids is ignored, possibly resulting in underestimation of the concentration of metals transported to recipient waters (Pédrot *et al.*, 2008). Furthermore, with future climate change, increased precipitation is expected in Sweden, some parts of Europe and the United States (Pachauri & Meyer, 2014). One potential effect of increased precipitation on the leaching of contaminants is enhanced mobilisation of particles and colloids to which contaminants might be adsorbed (Yin *et al.*, 2010). In addition, the dissolved concentration is assumed to be the <0.45  $\mu\text{m}$  fraction, but this fraction could contain colloids (Pédrot *et al.*, 2008). The solubility of elements in contaminated soils can also be governed by both sorption mechanisms and mineral dissolution (Scheckel & Ryan, 2004; Hashimoto *et al.*, 2011), making the solubility quite complex in some contaminated soils.

By considering the potential of the soil to leach particles and colloids in risk assessments, the total leaching of metal(loid)s might be assessed more accurately. Additionally, by studying the speciation of metal(loid)s enables more in-depth understanding of the leaching characteristics of metals in historically contaminated soils.



## 2 Rationale of thesis

When studying the transport and solubility of metals in contaminated soils, it is commonly only the partitioning between the bulk soil and the aqueous phase that is considered. The metals with high affinity for soil organic matter and iron (hydr)oxides are believed not to be very mobile in soils.

Particles and colloids transported in the soil can be both organic and inorganic. Particles and colloids with a high metal-adsorbing ability are mainly iron (hydr)oxides and organic colloids. Hence, metals that have high affinity for soil organic matter and iron (hydr)oxides have the potential to be transported with particles and colloids (Denaix *et al.*, 2001; Pédrot *et al.*, 2008). Thus, these elements might not be as immobile as partitioning between only the bulk soil and the aqueous phase might suggest.

One of the many consequences of the current changing climate is that increased frequency of high-intensity rainfall events is predicted for some parts of Europe and North America (Pachauri & Meyer, 2014). At high rainfall intensities, larger pores become filled with water (Lægdsmand *et al.*, 2005) and the shear stress might increase (Kaplan *et al.*, 1993; Bergendahl & Grasso, 2003), resulting in a higher potential for leaching of particles and colloids (Lægdsmand *et al.*, 1999; Lægdsmand *et al.*, 2005; Yin *et al.*, 2010). However, increased leaching of particles and colloids at increased rainfall intensity has not always been observed (Jacobsen *et al.*, 1997). This suggests that the effect of irrigation intensity on the leaching of particles and colloids might be soil-dependent. Moreover, the leached truly dissolved concentration, which is governed by equilibrium processes, could possibly be affected by the shorter water-soil-contact times at higher rainfall intensities, as some metals have slow reaction kinetics (Gustafsson *et al.*, 2014; Kim *et al.*, 2015).

Several studies show the importance of colloid-mediated transport of metals from contaminated soils (*e.g.* Denaix *et al.*, 2001; Pédrot *et al.*, 2008) and the importance of including these processes in risk assessments of contaminated soils (Denaix *et al.*, 2001; Klitzke *et al.*, 2012). However, detailed information

about the characteristics and solubility of metals adsorbed to particles and colloids is scarce. Moreover, as the major phase of a soil is the bulk soil, and not the mobile phase, it is of the utmost importance to study the leaching mechanisms, speciation and solubility for elements in the bulk soil, along with the leaching of particles and colloids.

In this thesis work, I sought to test the assumptions made in risk assessments today and to bring new insights on the processes controlling the transport of metal(loid)s in historically contaminated soils. A conceptual diagram of the assumptions made in standard risk assessments today, in comparison with the actual potential processes governing the leaching of metals in soil, is presented in Figure 1. My intention with this thesis work was to increase current knowledge on transport processes of metal(loid)s in historically contaminated soils, including solubility control mechanisms of dissolved species, as well as particle- and colloid-facilitated transport in dynamic systems. How the overall transport might be affected by increased rainfall intensity was of particular interest. Furthermore, to connect with the world outside academia, three standardised leaching tests commonly used in risk assessments were tested and evaluated in relation to more realistic field-like conditions, using size-based elemental fractionation.

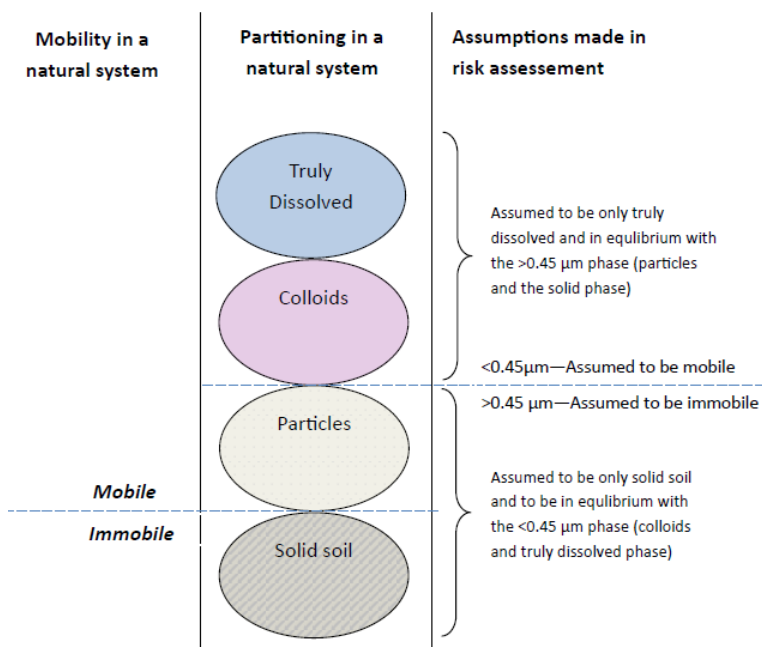


Figure 1. Comparison between the mobility and partitioning of different size fractions leached in soil solution and the simplified assumptions made in risk assessments (modified from Elert *et al.*, 2006).

### 3 Aim

The overall aim of this thesis work was to advance knowledge on processes controlling the solubility and transport of metal(loids) in historically contaminated soils, with the focus on particle- and colloid-mediated transport.

Specific objectives were to:

- Assess the speciation and solubility of lead and chromium in the bulk soil and in particles and colloids leached from historically contaminated soils (Papers I, II and III).
- Study the magnitude of particulate, colloidal and truly dissolved transport of lead, chromium, zinc, arsenic and antimony in intact soil columns (Papers II, III and IV).
- Study the effect of increased rainfall intensity on transport of particulate, colloidal and truly dissolved fractions of lead and chromium in intact soil columns (Papers II and III).
- Evaluate, using size-based elemental fractionation, the ability of three standard leaching tests to assess the leaching of lead, zinc, arsenic and antimony from intact soil columns (Paper IV).



## 4 Structure of thesis

Processes governing the leaching of metal(loid)s from four historically contaminated soils were at the core of this thesis work. The research comprised experiments performed on intact columns of these four soils. The methods used are explained briefly in Chapter 5 and are described in detail in Papers I-IV. Throughout the remainder of the thesis, relevant literature on each specific topic is presented together with empirical results obtained in the experiments.

Chapter 6 begins by describing the chemical and physical bulk soil properties of the four historically contaminated soils, followed by a presentation of the hydraulic properties of the intact soil columns.

Next, the solubility and speciation of lead, chromium, zinc, arsenic and antimony in the bulk soils are discussed, although greater emphasis is placed on the speciation and solubility of lead and chromium.

Once the processes governing metal solubility in bulk soil have been explained, the mechanisms of particulate (0.45 to 50  $\mu\text{m}$ ), colloidal (10 kDa to 0.45  $\mu\text{m}$ ) and truly dissolved (<10 kDa) leaching of metal(loid)s in intact soil columns are described. Natural colloids, potential carriers of metals, are discussed first, and the speciation of iron in leached particles and colloids is evaluated. The partitioning of lead, chromium, zinc, arsenic and antimony is then considered, again with the main emphasis on lead and chromium. The effect of irrigation intensity on metal leaching is discussed and the speciation of lead and chromium in the leached particles and colloids is described.

Having identified the leaching mechanisms in the four contaminated soils, the potential of three standard leaching test to predict leaching of lead, chromium, zinc, arsenic and antimony from intact soil profiles is assessed.

Finally, some conclusions are drawn from the experimental results and the implications of the novel insights gained into solubility control mechanisms and the role of particle- and colloid-facilitated transport of metals in contaminated soils are assessed. As a final synthesis of the research findings, a work-flow process for improved risk assessments is presented.



## 5 Methods

In this work, intact soil columns from four historically contaminated soils were used to study the transport mechanisms of metal(loid)s. The methods described below were applied to all four soils, unless otherwise stated. Information on the paper in which the different methods were used, where more information about the methods can be found, is provided in Table 1.

Table 1. *Overview of methods and papers where they were used.*

Method	Paper I	Paper II	Paper III	Paper IV
Sampling methods and history of soils	x	x	x	x
Irrigation experiment		x	x	x
Hydraulics of intact soil columns		x	x	x
EXAFS	x	x	x	
Geochemical modelling	x	x	x	
pH-dependent solubility batch test	x		x	
Time-dependent solubility batch test	x		x	x
Standardised leaching tests				x

### 5.1 Study sites and sampling of intact soil columns

The industrial activities at the historically contaminated sites lasted from 1905 to 1955 at Åsbro (wood impregnation), from 1871 to 1977 at Pukeberg (glass works), from 1860 to 1960 at Vinterviken (chemical industry), and from 1936 to 1995 at Gyttorp (shooting range), and are all located in Sweden (Figure 2). More information can be found in Supporting Information to Paper I.

Three or four intact soil columns ( $\varnothing=20$  cm, depth=30 cm, starting at the soil surface) were collected at each of the four sites. A plastic pipe ( $\varnothing=20$  cm) was pushed into the soil (Figure 2). The columns were cut to the right length and carefully prepared in the laboratory before the irrigation experiment.



Figure 2. Location of study sites and sampling of intact soil columns. The map shows the southern half of Sweden.

## 5.2 Irrigation experiment

The intact soil columns were used in an irrigation experiment performed with artificial rain water (ionic strength 0.055 mM, pH 5) (SMHI, data hosting), under unsaturated flow conditions in an irrigation chamber (Liu *et al.*, 2012) allowing free drainage at the base. Polyamide cloth (mesh size 50  $\mu\text{m}$ ) was attached to the bottom of the columns. The soil columns were conditioned with an irrigation intensity of 2  $\text{mm h}^{-1}$  until the electrical conductivity of the leachate remained constant. To study the effect of increased irrigation intensity, three different irrigation intensities were applied (2, 10 and 20  $\text{mm h}^{-1}$ ) and then a 2  $\text{mm h}^{-1}$  session was applied again at the end to study the recovery of leached concentrations from the higher irrigation intensities. The last irrigation session of 2  $\text{mm h}^{-1}$  was not applied in the experiment with the Åsbro soil. At each irrigation intensity, the leachate was sampled three to five times between 0.4-6.5 effective pore volume ( $\text{PV}_{\text{eff}}$ ), *i.e.* the volume of pores actively participating in transport calculated from non-reactive tracer breakthrough curves (BTC). To study the extent of particulate and colloidal leaching, the leachate was analysed in three size fractions: particles (0.45 to 50  $\mu\text{m}$ ), colloids (10 kDa to 0.45  $\mu\text{m}$ ) and truly dissolved (<10 kDa) (Figure 3).

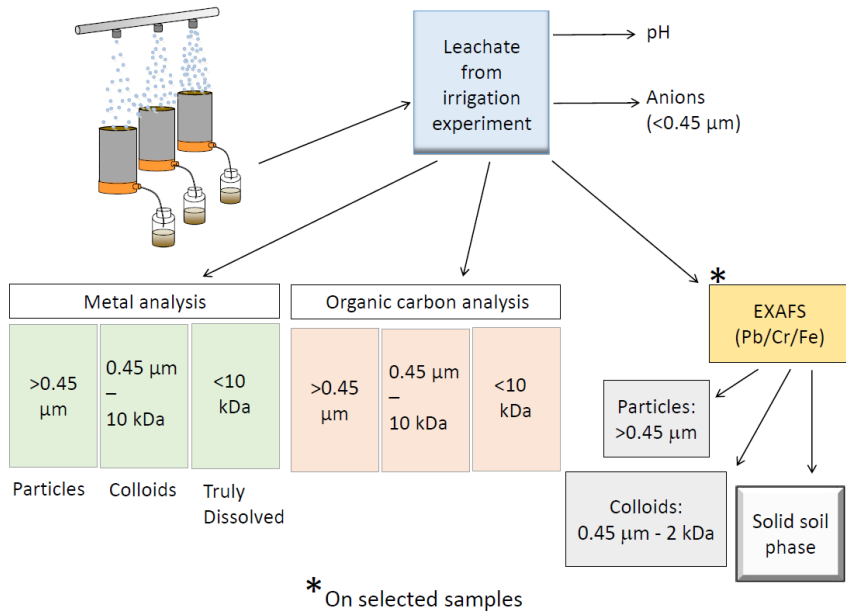


Figure 3. Flowchart for sample handling during the irrigation experiment.

### 5.3 Soil physical characterisation

Prior to use in the irrigation experiment, X-ray tomography (XRT) images of the intact soil columns were taken using a GE Phoenix v|tome|x m instrument. The X-ray tomography images were used to study the general characteristics of the pore system, potential layering in the soil and whether and to what extent extraction of the columns might have affected the soil structure.

Non-reactive tracer transport was studied by applying deuterium, at all three irrigation intensities in the irrigation experiment. A breakthrough curve (BTC) was constructed and from the BTC the extent of macropore flow (5 % arrival time), contact time and  $PV_{\text{eff}}$  were calculated according to Koestel *et al.* (2011). The unsaturated hydraulic conductivity was measured using infiltrometer measurements on intact soil columns at pressure potential of -1 cm, -5 cm and -10 cm, assuming vertical flow only (Klute & Dirksen, 1986). Soil texture was analysed using the pipette method devised by Gee and Bauder (1986).

### 5.4 Size-based fractionation of elements

As a first step in the speciation analysis, leachate from the irrigation experiment was fractionated into three different size fractions: particles 0.45 to 50  $\mu\text{m}$ ; colloids 10 kDa to 0.45  $\mu\text{m}$  and truly dissolved <10 kDa. This was done in order

to quantify the tendency for the different elements to be transported with particles and colloids or in truly dissolved form. The 0.45  $\mu\text{m}$  cut-off was chosen because this is a commonly used value in standardised leaching tests. The use of <10 kDa fractions allows dissolved fulvic acids to pass through to the truly dissolved fraction, whereas most colloidal iron/aluminium (hydr)oxides will not pass through (Wilkinson & Lead, 2007).

For the particles and colloids analysed with extended X-ray absorption fine structure (EXAFS) spectroscopy (described in section 5.5), the particles in leachate were immobilised by filtration over a 0.45  $\mu\text{m}$  filter, using an inline filter holder. The filtrate that passed through this filter was concentrated 5- to 10-fold using a crossflow ultrafiltration system with a cut-off of 2 kDa. The concentrated solution containing colloids was freeze-dried.

## 5.5 EXAFS

Extended X-ray absorption fine structure (EXAFS) spectroscopy was performed in the synchrotrons Maxlab II in Lund, Sweden, and SSRL, United States. Measurements were performed on both the bulk soil and the particles and colloids leached in the irrigation experiment (Table 2). No pre-treatment of samples is needed and measurements can be performed on fresh samples. Using this method, information can be obtained on the oxidation state and intra-molecular structure, such as identification of atoms, number of atoms and distances to neighbouring atoms. When evaluating EXAFS data, a shell-by-shell model is constructed (Kelly *et al.*, 2008). Hereafter, the shell-by-shell method is referred to as ‘shell fitting’. The programmes used for analysing experimental data were Athena (Ravel & Newville, 2005) and Artemis (Ravel, 2001; Ravel & Newville, 2005).

Wavelet transform analysis was also performed on the EXAFS data. Wavelet transform analysis enables visual discrimination in a graph (e.g. as in *Figure 14*) between elements of different atomic weight that are roughly the same distance from the absorbing atom (Funke *et al.*, 2005), which gives characteristic features to the graph (Karlsson & Persson, 2010; Gustafsson *et al.*, 2014).

Table 2. *Samples and elements analysed in bulk soil (Soil), particles (Part.) and colloids (Coll.) using extended X-ray absorption fine structure (EXAFS) spectroscopy*

	Åsbro			Pukeberg			Vinterviken			Gyttorp		
	Soil	Part.	Coll.	Soil	Part.	Coll.	Soil	Part.	Coll.	Soil	Part.	Coll.
Pb				x	x		x	x	x	x		x
Cr	x	x	x									
Fe	x	x	x	x	x		x	x	x	x		x

## 5.6 Time- and pH-dependent solubility

The solubility of lead, chromium, zinc, arsenic and antimony as a function of time, and the pH-dependent solubility of lead and chromium were studied in a series of batch experiments on soil materials (<2 mm) from the top and bottom layers of one representative column from each site. Field-moist soil was added to 0.01 M sodium nitrate solution at a liquid-to-solid ratio (L/S) of  $\approx 21$  on a dry weight basis. Nitric acid and sodium hydroxide were added to adjust the pH to within the range 2 to 8, depending on soil. For the pH-dependent solubility test, duplicate samples were shaken in darkness at 21 °C on an end-over-end shaker for five days. For the time-dependent solubility test, duplicate samples were shaken for 1, 5 and 32 or 33 days (and 61 and 90 days for chromium in Åsbro, only in paper III) at ambient pH and low pH (only for lead and chromium). The suspensions were centrifuged and filtered using 0.45  $\mu\text{m}$  syringe filters and 10 kDa ultra-centrifuge filters.

## 5.7 Geochemical modelling

Geochemical equilibrium models can be used to describe the speciation of a compound in different chemical environments. By applying different assumptions on soil properties in the model, the results from laboratory work can be explained on a molecular scale (*e.g.* Gustafsson *et al.*, 2014).

In this thesis work, Visual MINTEQ was used as the modelling tool. The programme is based on the assumption of chemical equilibrium. Visual MINTEQ contains a large database of equilibrium constants for various mineral phases that can be used to calculate saturation indices and, when applicable, the concentration of mineral precipitates. The adsorption of metal(loid)s by metal (hydr)oxides, soil organic matter (SOM, consisting of humic acid+fulvic acid (HA+FA)) and dissolved organic matter (DOM, consisting of FA) is described in sub-models incorporated into Visual MINTEQ.

In this thesis work speciation and solubility of lead and chromium was modelled in the bulk soil, as well as in the particles and colloids leached in the irrigation experiment. In the ‘generic model’ used in Papers I-III, the settings for active fraction of hydroxides, SOM and DOC were not optimized and precipitation of mineral phases was not considered. However, the saturation index of possible minerals should always be tested. In this work, assumptions commonly used in geochemical modelling was applied in the model and the outcome of the model was validated against EXAFS results and pH dependent solubility tests. The assumptions made for adsorption sites in the ‘generic models’ are presented in Table 3. For detailed information about the assumptions made in the ‘generic model’ the reader should consult Papers I-III (Table 1).

Table 3. Assumptions made in the 'generic model' setups for adsorption sites. SOM = soil organic matter, TOC = total organic carbon, DOM = dissolved organic matter, DOC = dissolved organic carbon, HA = Humic acid, FA = Fulvic acid, Fe = iron, Al = aluminium.

	Bulk soil	'Colloids plus particles'
Solid SOM	[SOM] = 2 * [TOC] 25 % of solid SOM = HA 25 % of solid SOM = FA	[SOM] = 2 * ([OC] in 10 kDa to 50 $\mu$ m fraction) 25 % of solid SOM = HA 25 % of solid SOM = FA
Hydroxides	Oxalate extracted [Fe <sub>ox</sub> ] and [Al <sub>ox</sub> ] corrected for complexation to SOM using Minteq. Specific surface area, 650 cm <sup>2</sup> g <sup>-1</sup> for lead and 600 cm <sup>2</sup> g <sup>-1</sup> for chromium*.	Fe+Al conc. in 10 kDa to 50 $\mu$ m fraction corrected for complexation to SOM using Minteq. Specific surface area, 350 cm <sup>2</sup> g <sup>-1</sup> for both lead and chromium.
DOM (<10 kDa)	[DOM] = 2 * [DOC] [DOM] = [FA]	[DOM] = 1.65 * [DOC] [DOM] = [FA]

\*Different sorption models were used for lead and chromium.

## 5.8 Standardised leaching tests

To study how well the leaching tests used in risk assessments describe the leaching of lead, zinc, arsenic and antimony from intact soil columns, one percolation test using repacked soil columns, and two batch tests were evaluated. In the common experimental set-up, only the concentration in the <0.45  $\mu$ m fraction is considered and it is assumed that this concentration is in equilibrium with the bulk soil concentration. If substantial particle-facilitated transport of contaminants is expected, an 8  $\mu$ m filtration is recommended in the standard for the percolation test. In the experimental set-up used in Paper IV, the same cut-offs as in the irrigation experiment were used; for particles (0.45-8  $\mu$ m, only percolation test, however in the irrigation experiment the upper cut-off was set to 50  $\mu$ m), colloids (10 kDa to 0.45  $\mu$ m) and the truly dissolved fraction (<10 kDa). A summary of the experimental set-up is provided in Table 4.

Table 4. Experimental set-up used for the standardised leaching tests

	Percolation test	H <sub>2</sub> O batch test	CaCl <sub>2</sub> batch test
Name of standard test	CEN/TS 14405	EN 12457-2	ISO/TS 21268-2
Leachant	Deionised water	Deionised water	1 mM CaCl <sub>2</sub>
Agitation	None	Shaking	Shaking
Sample mass/volume	~500 g in 5*30 cm cylinder	95-125 g	95-125 g
Liquid-to-solid ratio	0.5, 2 and 10	10	10
Fraction analysed	<10 kDa, <0.45 $\mu$ m, <8 $\mu$ m	<10 kDa, <0.45 $\mu$ m	<10 kDa, <0.45 $\mu$ m
Contact time (hours)	21-29	24	24

## 6 Bulk soil properties

### 6.1 Chemical properties of experimental soils (Paper I-IV)

The texture and organic carbon content varied between the four soils studied in this thesis. The pH value ranged between 5.5 and 8 and the organic carbon content between 1 and 5 % (Table 5). The soils were classified as sandy loam (Åsbro and Vinterviken), sand (Pukeberg) and silty loam (Gyttorp) (Figure 4).

Table 5. *Properties of the contaminated bulk soils used in this study. Average concentrations for each site, with standard error of the mean (SEM) in brackets. OC = organic carbon, Fe = iron, Mn = manganese, Pb = lead, Cr = chromium, Zn = zinc, As = arsenic, Sb = antimony.*

Property	Units	Åsbro, wood impregnation	Pukeberg, glassworks	Vinterviken, industry	Gyttorp, shooting range
Sand	%	68.0 (0.8)	89.0 (0.62)	63.8 (0.40)	43.5 (0.28)
Silt	%	27.1 (0.8)	7.93 (0.52)	25.6 (0.40)	52.6 (0.22)
Clay	%	5.09 (0.21)	3.10 (0.15)	10.7 (0.22)	4.03 (0.10)
pH	%	6.44 (0.07)	7.90 (0.01)	5.52 (0.03)	5.56 (0.07)
OC	%	5.15 (0.25)	1.37 (0.23)	3.97 (0.19)	1.73 (0.03)
Fe	mg kg <sup>-1</sup>	12 100 (630)	5 740 (1020)	13 700 (448)	6 300 (125)
Mn	mg kg <sup>-1</sup>	1 090 (90.6)	216 (27.4)	309 (13.4)	70.0 (2.34)
Pb	mg kg <sup>-1</sup>	897 (268)*	356 (66.2)*	551 (134)*	2 220 (310)*
Cr	mg kg <sup>-1</sup>	1 110 (55.5)*	6.59 (2.62)	17.3 (1.0)	4.33 (0.10)
Zn	mg kg <sup>-1</sup>	2 500 (89.9)*	309 (40.3)*	123 (6.36)	17.0 (1.46)
As	mg kg <sup>-1</sup>	2 710 (117)*	33.7 (3.91)*	6.61 (0.62)	28.6 (18.2)*
Sb	mg kg <sup>-1</sup>	8.48 (0.97)	30.0 (4.80)*	3.83 (1.14)	18.6 (2.33)*

\*The concentration exceeds the Swedish guideline value for 'sensitive soil use' (*känslig markanvändning*, KM), which means that adults and children cannot reside in the area permanently, *e.g.* this area cannot be used as a residential area (Swedish EPA, 2009).

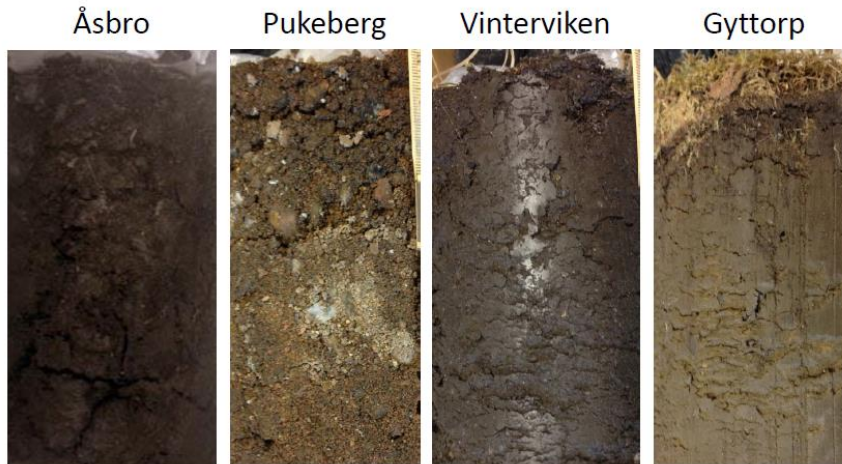


Figure 4. Picture of intact columns of the four soils after the irrigation experiment.

Detailed descriptions of soil properties in risk assessment reports is commonly quite poor. However, amongst the risk assessments from which the four soils used in this thesis work was chosen, 10 more risk assessment reports were found where the texture, pH and organic carbon content in bulk soil was analysed (Table 6). In these 10 soils the texture was often referred to as (coarse-grained) ‘filling material’, the pH ranged mainly from 5.3-9 and the organic carbon content, when given, was lower than 9 % and commonly <5 %. The soils used in this thesis work falls within the same pH-, organic carbon content- and texture-range as the soils in the survey.

Table 6. Ten risk assessment reports in which the texture, pH and organic carbon content in bulk soil was analysed. N.A. = not available.

Site	Texture	% OC	pH
Boxholms sawmill	25-37 % <0.05 mm.	0.5-2.2	7.7-8.8
Domsjö industry	Filling material	N.A.	N.A.
Igelstatomten, sawmill	Filling material	<1.7 mg l <sup>-1</sup> in soil leachate	N.A.
Floda, tannery	Filling material	3.5 to 9.1 %.	7.9-8.4
Nordbäcks wood	Filling material	<1 % in filling material	5.3-7.1
Surahammars industry	Filling material	N.A.	6.9-11
Österbyverken, metal industry	Filling material	N.A.	N.A.
Kagghamra, impregnation	<5 % clay	N.A.	6.2-9
Lessebo sawmill	Filling material	2.7-9.1 %	6-6.4
Lundbergs tannery	Filling material	N.A.	N.A.
Munkhyttan shooting range	Filling material	N.A.	N.A.

## 6.2 Hydraulic properties of experimental soils (Papers II and III)

Infiltration of water into the soil can be non-uniform and, when this occurs, the term preferential flow is commonly used (Hendrickx & Flury, 2001). This preferential flow occurs in the larger macropores and may result in non-equilibrium mass movement and accelerate movement of matter (Vogel *et al.*, 2007; Allaire *et al.*, 2009).

The breakthrough curves from the irrigation experiment for the four soils had a bell shape, with only small differences in shape and tailing of the curves between the irrigation intensities, indicating no extensive preferential flow (Figure 5). This is in agreement with the small decrease in 5 % arrival time at higher irrigation intensities (Table S3 in Paper II, calculated from BTC in Papers II and III). In addition, the XRT images revealed that all four soils lacked large continuous macropores and well-defined layering (Figure 6). The imaging indicated that some artificial macropores were created along the column walls during sampling. However, the results from the infiltrometer measurements suggested that the water flow through the columns was unsaturated for all soils and all three irrigation intensities (Figure S4 in Paper II), and the BTC indicated no extensive preferential flow. Hence, the artificial macropores created at sampling were air-filled during the irrigation experiments and only had a minor influence on the transport. Because of the porous and fairly homogeneous soil structure, the soils can be considered non-macroporous.

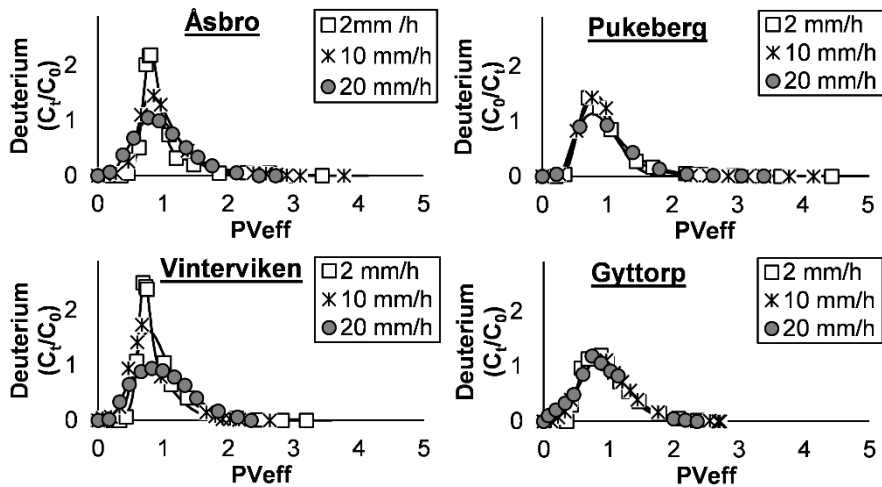
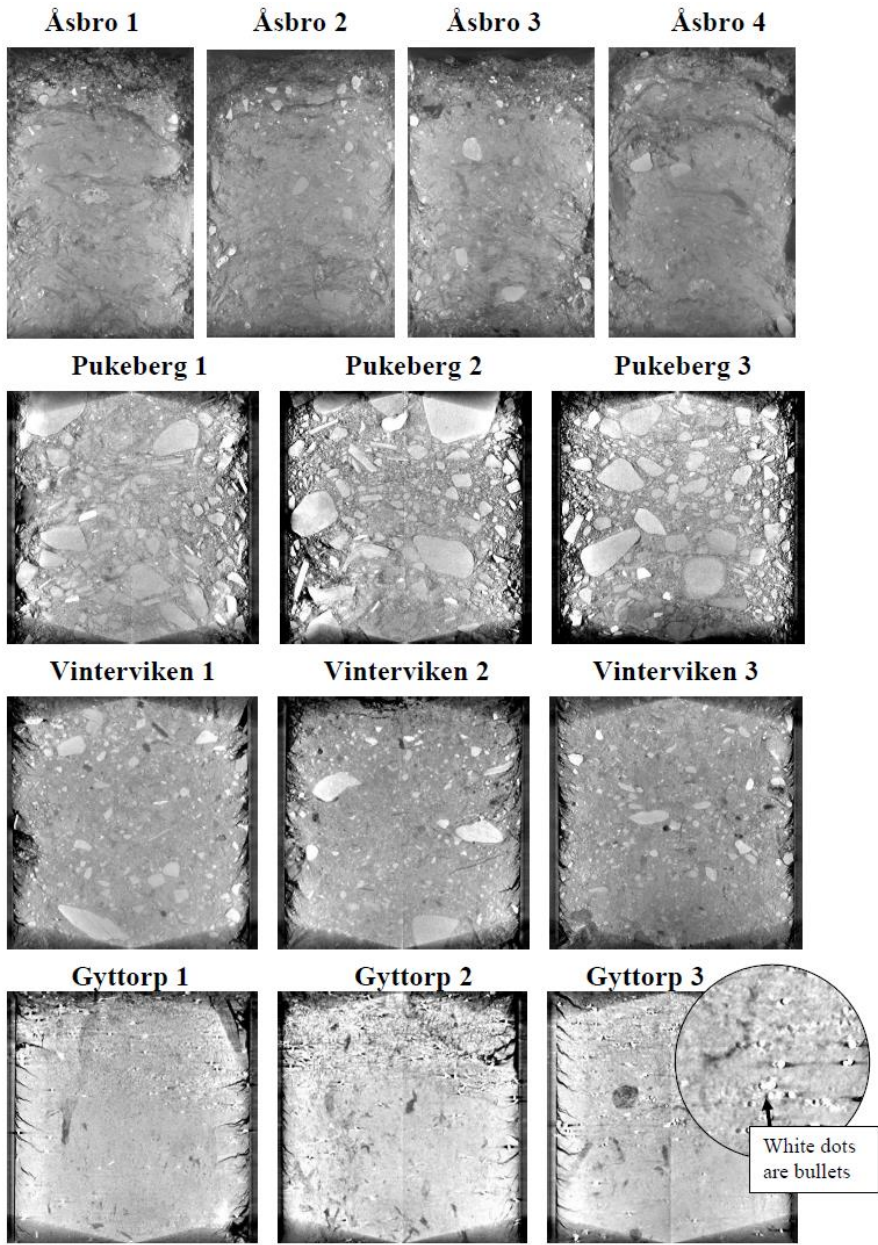


Figure 5. Breakthrough curves (BTC) at three different irrigation intensities for the four soils studied. One representative column from each soil is shown in this diagram, while the curves for all columns are shown in Figure S3 in Paper II.



*Figure 6.* X-ray tomography images of the columns used in the irrigation experiment. The images were taken before the irrigation experiment. Bright areas indicate high density and dark areas indicate low density.

## 7 Metal solubility and speciation in bulk soil

The speciation of an metal(loid) in bulk soil governs its solubility. The solubility of metal(loid)s in contaminated soils may be complex, as the solubility of an element can be governed by both mineral phases and sorption processes (Scheckel & Ryan, 2004; Hashimoto *et al.*, 2011). For metal(loid)s with high affinity for soil organic matter and hydroxides, fairly high concentrations of metals can be present before they precipitate.

The truly dissolved concentration (<10 kDa) of metal(loid)s in the soil leachate was measured in this thesis (Figure 7). By measuring the truly dissolved concentration, a well-defined fraction which can be used for calibration and/or validation of geochemical models describing the solubility of an element was obtained. The term solubility control mechanism refers to the solid phase reaction mechanism controlling the concentration of the free metal ion.

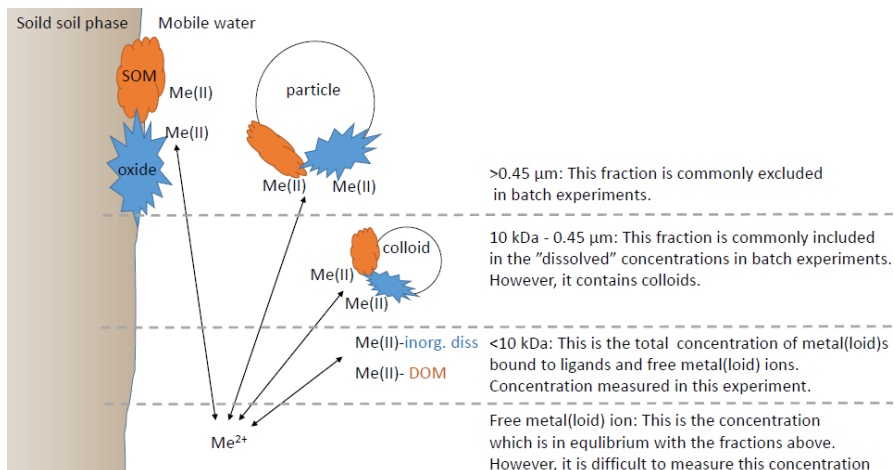


Figure 7. Illustration of the fractions usually analysed in batch experiments and the fraction analysed in this thesis, as well as the free metal ion fraction.

Results on the time-dependent solubility of lead, chromium, zinc, arsenic and antimony obtained from batch tests performed over 32-33 days are presented below. In addition, a thorough evaluation of solubility and speciation was performed on lead and chromium in this thesis.

## 7.1 Time-dependent solubility at ambient pH of lead, chromium, zinc, arsenic and antimony (Papers I and III-IV)

Lead, zinc and arsenic equilibrated fast in all four soils, as no consistent time trend was observed. However, sample heterogeneity resulted in large variations between some replicates, causing some variability between the different time points (Figure 8). Chromium in the Pukeberg, Vinterviken and Gyttop soils seemed to equilibrate within one day. However, in the Åsbro soil there was an increasing time trend between days 1 and 5, but after five days the concentration remained constant. Antimony in Vinterviken and Gyttop soil seemed to equilibrate within one day, whereas an increasing time trend was indicated in the glassworks soil, Pukeberg (see also Table 1 in Paper IV). This might be explained by slow weathering of glass. This slower leaching of antimony in Pukeberg soil could be considered biphasic (Kim *et al.*, 2015), since dissolution of the adsorbed fraction is fast, while dissolution of the glass phase is slow.

Hence, 24 hours seems to be long enough to reach conditions near equilibrium between the truly dissolved concentration and the bulk soil for sorbed metal(loid)s and rapidly reacting secondary minerals.

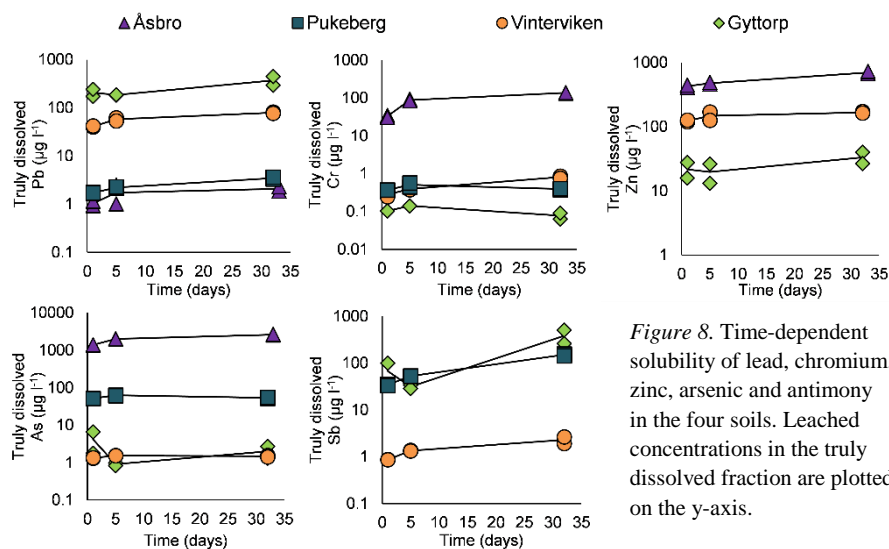


Figure 8. Time-dependent solubility of lead, chromium, zinc, arsenic and antimony in the four soils. Leached concentrations in the truly dissolved fraction are plotted on the y-axis.

## 7.2 Solubility and speciation of lead (Paper I)

In previous studies, lead in contaminated soils has been found in various mineral phases, such as precipitated mixed phases of litharge ( $\alpha$ -PbO) (Manceau *et al.*, 1996; Vantelon *et al.*, 2005), massicot ( $\beta$ -PbO) (Manceau *et al.*, 1996), PbCl<sub>2</sub>, PbSiO<sub>3</sub> (Manceau *et al.*, 1996) and/or anglesite (PbSO<sub>4</sub>) (Lin *et al.*, 1995; Manceau *et al.*, 1996) or as co-precipitates of anglesite and galena (PbS) (Scheckel & Ryan, 2004), hydrosocersite (Pb<sub>3</sub>(CO<sub>3</sub>)<sub>2</sub>(OH)<sub>2</sub>) and cerussite (PbCO<sub>3</sub>) (Lin *et al.*, 1995; Vantelon *et al.*, 2005). However, lead also has high affinity for soil organic matter and hydroxides (Manceau *et al.*, 1996; Scheckel & Ryan, 2004; Hashimoto *et al.*, 2011), indicating that lead might also frequently be present adsorbed to organic matter and hydroxides in contaminated soils.

In this thesis work, to assess the speciation of lead in the bulk soil, EXAFS measurements were performed on the Pukeberg, Vinterviken and Gyttop soils. It was not possible to perform EXAFS measurements on the Åsbro soil because of the high arsenic background interfering with the L<sub>3</sub>-edge fluorescence signal.

By performing shell fitting, a Pb-O distance between 2.29-2.39 Å was identified in all three soils. This proposes a coordination number (CN) of 3-4, because the bond distance distribution for CN=3 and 4 is very wide (2.22-2.46) (Persson *et al.*, 2011; Bajnóczi *et al.*, 2014). This Pb-O distance also indicates that lead was adsorbed to a surface such as soil organic matter, ferrihydrite or aluminium hydroxide (more information on lead coordination chemistry can be found in Supporting Information to Paper II).

In the Vinterviken and Gyttop soils, the EXAFS spectra resembled that of the Pb-Fulvic acid standard (Figure 9). Furthermore, a Pb-C contribution was successfully added at 3.23-3.31 Å, suggesting that the major phase was lead bound to soil organic matter in these two soils. For the Pukeberg soil no second shell was successfully added, but some features of its spectrum resembled that of the Pb-aluminium hydroxide standard. However, it should be remembered that Pukeberg soil is a glassworks soil and might consist of a mixture of soil and pieces of glass.

The ability of geochemical modelling programme Visual MINTEQ to describe the lead speciation in the solid phase was tested. The 'generic model' assumptions (50 % active SOM and 100 % active hydroxides, and not allowing for lead mineral precipitation), gave good predictions of the lead solubility. However, to retrieve a better prediction of the lead speciation, the fraction of 'active' Al+Fe hydroxides and soil organic matter was varied between 0-100 % and 50-100 %, respectively. Interestingly, the optimised models with the lowest root mean square error (RMSE) for the solubility prediction, were models that

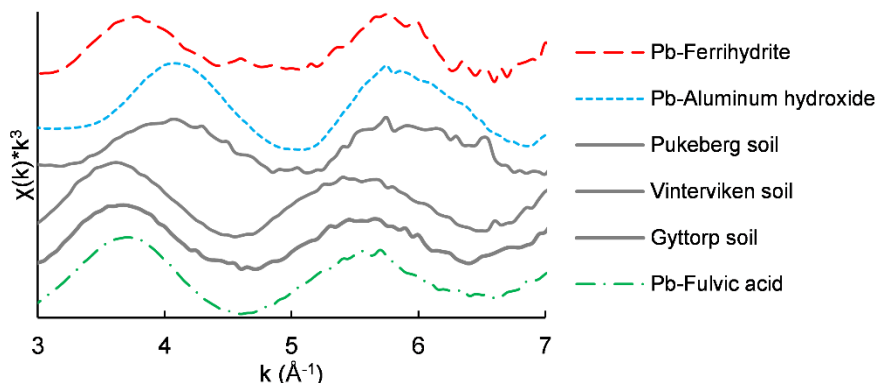


Figure 9. Lead  $L_3$  spectra for Pukeberg, Vinterviken and Gyttop bulk soils and for three lead standards: Lead adsorbed to ferrihydrite (Tiberg *et al.*, 2013), lead adsorbed to aluminium hydroxide (Tiberg *et al.*, 2018) and lead adsorbed to fulvic acid (Tiberg *et al.*, 2018).

gave speciation results corresponding better with the EXAFS speciation analysis than the ‘generic model’ (Figure 9 and Figure 10, and Figure 5 in Paper I).

Geochemical modelling provided interesting information on the speciation of lead in the arsenic-rich Åsbro soil. First, it was possible to suggest that the solubility was not governed by sorption to hydroxides and/or soil organic matter (‘generic model’ in Figure 10), and hence the solubility is most likely governed by dissolution of a mineral phase. Amongst the mineral phases tested, the best fit was found for mimetite ( $Pb_5(AsO_4)_3Cl$ ) (Figure 10), providing an ion activity product that was nearly constant over the whole pH range (Figure S4 in Paper I). The solubility product reported for mimetite in the literature varies and the value chosen for Åsbro was taken from a study where the mimetite was aged for 14 weeks (Inegbemor *et al.*, 1989), probably resulting in a more crystalline form than in other studies (Bajda, 2010). The contaminants in Åsbro have been aged for a long time (>60 years), thus probably forming a more crystalline form of mimetite.

This difference in lead species between different soils corresponds well with previous findings (*e.g.* Manceau *et al.*, 1996; Scheckel & Ryan, 2004; Hashimoto *et al.*, 2011). Since the speciation varies a good deal between soils, it is important to obtain some knowledge on what governs the solubility when *e.g.* performing a risk assessment. As EXAFS is an advanced technique requiring a synchrotron for measurements and experience in evaluating the data, it is not an option for speciation analysis in standard risk assessments. However, as illustrated for lead, by performing a pH-dependent solubility test (and assessing the truly dissolved concentrations, <10 kDa) in combination with

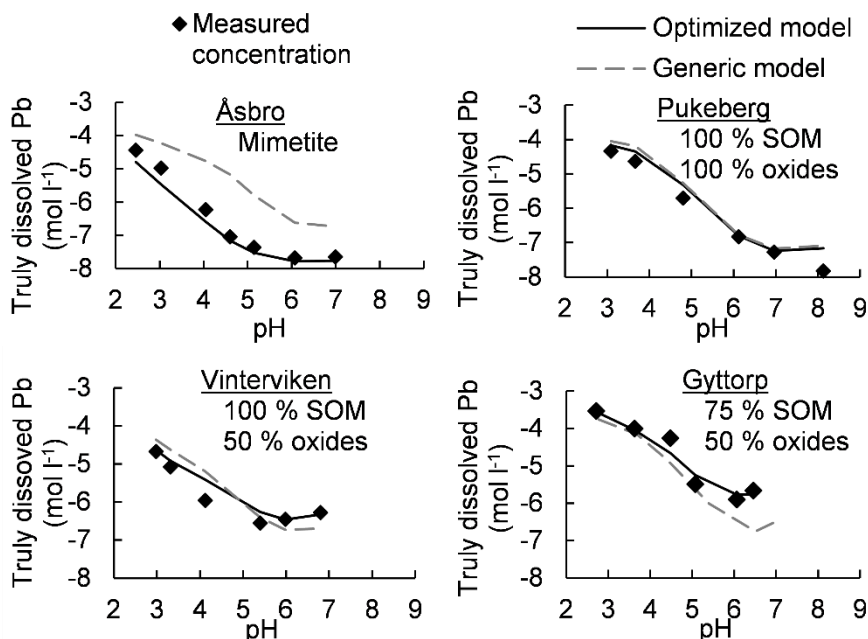


Figure 10. The pH-dependent solubility of lead in the bulk soil in Åsbro, Pukeberg, Vinterviken and Gyttorp. The y-axis shows leached and modelled concentrations in the truly dissolved fraction (<10 kDa) and is plotted on log-scale. The percentages of soil organic matter (SOM) and oxides given in the graphs are the optimised models with the lowest root mean square error (RMSE). The ‘generic model’ was set to 50 % active SOM and 100 % active oxides.

geochemical modelling, it is possible to determine whether the solubility of a metal is governed by sorption processes or by dissolution of a mineral in a contaminated soil.

### 7.3 Solubility and speciation of chromium (Paper III)

The two most common oxidation states of chromium in soils are chromium(III) and chromium(VI). The oxidised chromium(VI) is considered to be more toxic and is stable in “pure” oxic aqueous solutions (Ball & Nordstrom *et al.*, 1998). However, soil organic matter can reduce chromium(VI) to chromium(III) under oxic conditions (Wittbrodt & Palmer, 1996; Jardine *et al.*, 1999; Tokunaga *et al.*, 2001).

In previous studies on contaminated soils, chromium has mainly been found as chromium(III) precipitates, such as co-precipitates of chromium(III) and iron(III) hydroxides (Delsch *et al.*, 2006; Hopp *et al.*, 2008; Elzinga & Cirno, 2010), chromium(III) hydroxides (Delsch *et al.*, 2006; Ding *et al.*, 2016) and chromite (FeCr<sub>2</sub>O<sub>4</sub>) (Peterson *et al.*, 1997; Delsch *et al.*, 2006; Elzinga & Cirno,

2010; Landrot *et al.*, 2012). However, because of the high affinity of chromium(III) to soil organic matter (Wittbrodt & Palmer, 1996; Gustafsson *et al.*, 2014) and iron (hydr)oxides (Stumm, 1992), fairly high concentrations of chromium(III) might exist in the soil before chromium mineral precipitation.

In this work, a speciation analysis was performed on the Åsbro soil using both EXAFS and geochemical modelling. The EXAFS measurements suggested that the chromium in Åsbro soil was present as chromium(III) in the solid soil (Figure S5 in Paper III). Precipitation of  $\text{Cr}(\text{OH})_3$  ( $K_s=9.35$ ) and  $\text{Cr}_2\text{O}_3$  ( $K_s=8.52$ ) was excluded based on the shape of the EXAFS spectra for  $\text{Cr}(\text{OH})_3$  (Figure 11), and on calculated saturation indices using Visual MINTEQ (Table S8 in Paper III).

Shell fitting suggested that chromium(III) was coordinated to six oxygen atoms at  $\approx 1.98$  Å in an octahedral configuration, which was confirmed by a multiple scattering path ( $\approx 3.9$  Å). In addition, a Cr··Cr distance at 2.93-3.0 Å, in accordance with a dimeric structure (Gustafsson *et al.*, 2014), was identified (Figure 11). The presence of a potential Cr··Fe distance was excluded, since the Cr··Fe distance was found to be longer, 3.07 Å (Table S4 in Paper III). The general formula of the chromium(III) dimer is  $[\text{Cr}_2(\text{OH})_2(\text{H}_2\text{O})_{8-x}\text{L}_x]^{(4-x)}$ , where L is a ligand possibly consisting of a hydroxide, carboxyl or other oxygen or nitrogen donor ligand, most likely an organic ligand (Gustafsson *et al.*, 2014).

To further test the hypothesis that chromium in the Åsbro soil is governed by the solubility of dimeric chromium(III) complexes, a ‘generic model’ was set up in Visual MINTEQ. The set-up of the model is described in full in Paper III. Gustafsson *et al.* (2014) added a dimeric chromium(III)-SOM and a monomeric chromium(III)-SOM complex to Visual MInteq to describe the solubility and speciation of chromium(III) in an organic-rich soil to which chromium(III) salt had been added in the laboratory.

As illustrated in Figure 12, the model was able to describe the solubility of chromium in the Åsbro soil over the whole pH range, further strengthening the conclusion on presence of dimeric chromium(III)-SOM complexes in this soil. Moreover, at lower pH monomeric chromium(III)-soil organic matter complexes were formed according to the geochemical model (Figure S9 and S10 in Paper III). This is consistent with the findings of Gustafsson *et al.* (2014), who confirmed the existence of monomeric chromium(III)-soil organic matter complexes at low pH values using EXAFS on an organic-rich soil.

In this thesis work, the same ‘generic model’ set-up as used on the Åsbro soil was applied on the Pukeberg, Vinterviken and Gyttop soils. First, amorphous  $\text{Cr}(\text{OH})_3$  and crystalline  $\text{Cr}_2\text{O}_3$  were not supersaturated according to Visual MINTEQ, suggesting that chromium had not precipitated in any of the four soils. Instead, the ‘generic model’ was able to describe the pH-dependent

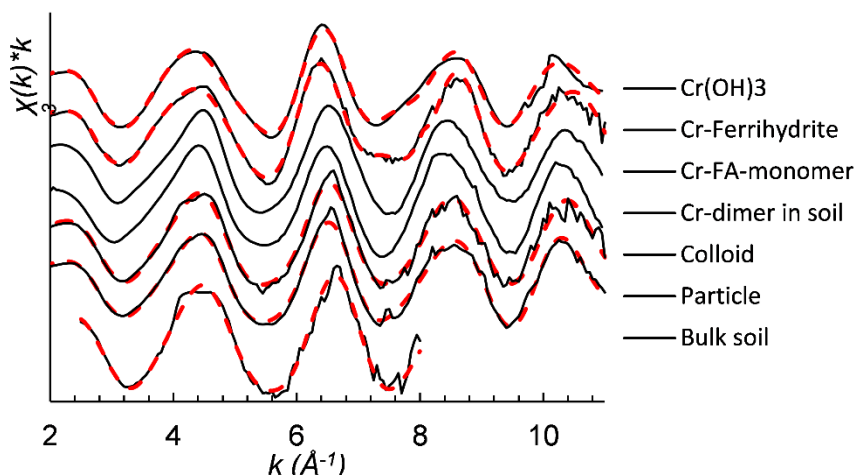


Figure 11. Stacked Cr(III)  $k^3$ -weighted K-edge extended X-ray absorption fine structure (EXAFS) spectra for Åsbro bulk soil and particles and colloids in that soil, and for amorphous chromium hydroxide ( $\text{Cr}(\text{OH})_3$ ), chromium adsorbed to ferrihydrite (Cr-Ferrihydrite), monomeric chromium adsorbed to fulvic acid (Cr-FA-monomer) and dimeric chromium (Cr-dimer) in an organic-rich soil (the last two from Gustafsson *et al.*, 2014).

solubility by using the dimeric and monomeric chromium(III)-soil organic matter complex in all four soils (Figure 12). This suggests that mainly dimeric chromium(III) was present in all four soils at ambient pH, and that this ‘generic model’ set-up could possibly be used as a tool in site-specific risk assessments.

Furthermore, Gustafsson *et al.* (2014) showed that when spiking an organic-rich soil with chromium(III) salt, the reaction kinetics at low pH are very slow, *i.e.* with  $\geq 90$  days needed to reach equilibrium. Therefore, it was important to study the time dependent solubility of chromium at low pH in the four contaminated soils. In Åsbro and Pukeberg the pH drifted throughout the time dependent solubility experiment, resulting in a decrease in concentration over time. However this decrease in truly dissolved concentrations fell exactly on the solubility data for the 5 days pH dependent solubility test (Figure 12). For the Vinterviken and Gyttop soils, the pH did not drift during the experiment, giving constant chromium concentrations over time. Accordingly, equilibration of chromium(III) seems to be fast in contaminated soils, including at low pH.

The time-dependent solubility test at low pH suggests that the transition from the stable dimeric chromium(III) at near neutral pH to the monomeric chromium(III) at low pH is fast. This is in contrast to the long ( $\geq 90$  days) equilibrium time observed by Gustafsson *et al.* (2014) on spiking an organic-rich soil with  $100 \mu\text{M}$  chromium(III). Hence, the cleavage rate of the hydroxyl bridge in the dimeric chromium(III) (Spiccia, 1991; Crimp *et al.*, 1994) and the

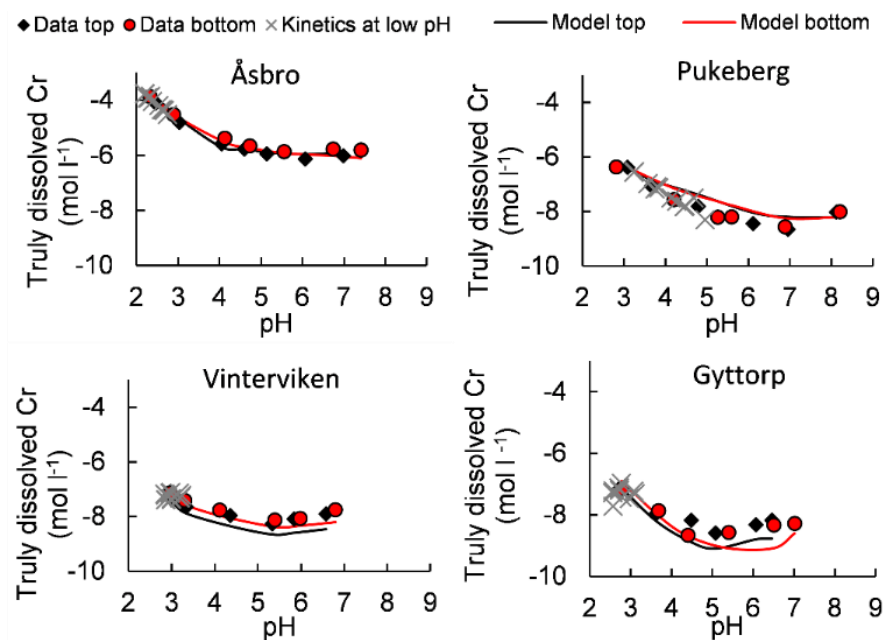


Figure 12. pH-dependent solubility of chromium in the top layer (black) and bottom layer (red) of Åsbro, Pukeberg, Vinterviken and Gyttorp soil columns. The grey Xs indicate the data from all time steps (1 to 32 or 33 days) in the time-dependent solubility test at low pH. The y-axis shows leached and modelled logged concentrations in the truly dissolved fraction (<10 kDa).

equilibration of the monomeric chromium(III) complex in soils is much faster than the water exchange rate (Xu *et al.*, 1985) for the freshly added chromium(III) ions.

In contrast to previous studies, where chromium has mainly been found as precipitates in contaminated soils (Peterson *et al.*, 1997; Delsch *et al.*, 2006; Hopp *et al.*, 2008; Elzinga & Cirimo, 2010; Landrot *et al.*, 2012), the data obtained in this thesis suggest that chromium occurred as a dimeric chromium(III)-SOM complexes in all four soils. Hence, under ambient conditions this dimeric chromium(III) complex seems to be thermodynamically stable, since it has existed in the soil for >60 years at Åsbro, even at the high concentrations of chromium found at that site (1100 mg kg<sup>-1</sup>).

## 8 Particle- and colloid facilitated transport of metals

Particles and colloids can be present in both organic and inorganic materials and they could play a leading role in the transport of metal(loid)s in soils and waters. Particles and colloids that readily adsorb metal(loid)s are (hydr)oxides and organic materials. Hence the partitioning of iron, aluminium, manganese and organic carbon could give an indication of the potential for particulate and colloidal transport of metal(loid)s (Pokrovsky *et al.*, 2006; Pédrot *et al.*, 2008; Klitzke *et al.*, 2012).

The size definition of particles and colloids varies between different studies (*e.g.* Denaix *et al.*, 2001; Zhang & Selim, 2007; Klitzke *et al.*, 2008; Pédrot *et al.*, 2008). For practical reasons, a size definition is needed in all experimental work. In this thesis, particles were defined as 0.45 to 50  $\mu\text{m}$ , colloids as 10 kDa to 0.45  $\mu\text{m}$  and the truly dissolved fraction as <10 kDa.

The following sections present the results on particle- and colloid-facilitated transport of iron, aluminium, manganese and organic carbon as well as the contaminating elements lead, chromium, zinc, arsenic and antimony obtained in the irrigation experiment using a rainfall intensity of 2  $\text{mm h}^{-1}$ . The 2  $\text{mm h}^{-1}$  intensity was chosen as this was the lowest irrigation intensity applied and can be viewed as a base flow. As intact soils were studied, although a large amount of water was applied compared with in natural conditions, the results on leaching of particulate, colloidal and truly dissolved fractions presented here can be assumed to be representative for field conditions (Gasser *et al.*, 1994).

## 8.1 Partitioning of iron, aluminium, manganese and organic carbon (Papers II-IV)

The particulate and colloidal fractions of iron in the Åsbro and Pukeberg soils comprised 85-97 % of the total amount of iron leached, while for the Vinterviken and Gyttop soils the corresponding figure was about 60 % (*Figure 13*). The size fractionation of aluminium was similar to that of iron. In the Åsbro soil, about 95 % of the total concentration of aluminium leached was found in the particle and colloidal fractions. In the Pukeberg and Vinterviken soils, the particle and colloidal fractions made up about 50-60 % of the total concentration of aluminium leached, whereas in Gyttop soil the proportion was about 40 %. The extensive particle and colloidal leaching of iron and aluminium is consistent with previous findings (Pokrovsky *et al.*, 2005; Pédrot *et al.*, 2008). For manganese, leaching with particles and colloids varies somewhat between the soils. Around 80 % of the total concentration of manganese was leached with particles and colloids in both the Åsbro and Pukeberg soils, and around 20-30 % in both the Vinterviken and Gyttop soils. This slightly lower tendency for manganese to be transported with particles and colloids is also in agreement with previous findings (Pédrot *et al.*, 2008).

Interestingly, leaching of organic carbon dominated in the truly dissolved fraction. Some organic carbon leached with particles and colloids only in the two soils with the highest total organic carbon content (4-5 %). In Åsbro soil, about 35 % of the total concentration of organic carbon in leachate was associated with (mainly) particles, while in Vinterviken soil about 20 % was leached in the colloidal fraction. However, the lower tendency for organic carbon to be transported with particles and colloids compared with iron, aluminium and manganese is in agreement with previous findings (Pokrovsky *et al.*, 2005; Pédrot *et al.*, 2008).

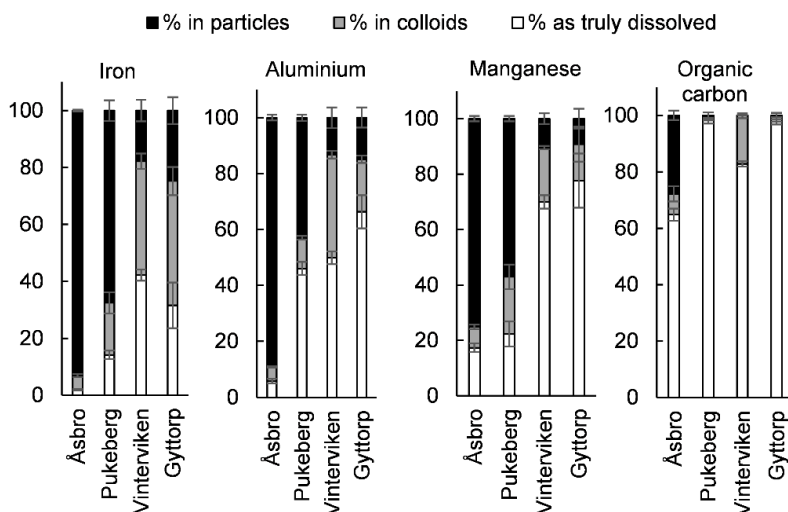


Figure 13. Particulate (0.45 to 50  $\mu\text{m}$ ), colloidal (10 kDa to 0.45  $\mu\text{m}$ ) and truly dissolved (<10 kDa) leaching of iron (Fe), aluminium (Al), manganese (Mn) and organic carbon from the four soils at irrigation intensity 2  $\text{mm h}^{-1}$ .

Overall, the results suggest that elements which have a high affinity for (hydr)oxides could potentially undergo major particle and colloidal mobilisation in all four soils. However, elements that are mainly bound to soil organic matter would most likely only be transported with particles and colloids in the Åsbro and Vinterviken soils.

### 8.1.1 Speciation of iron in bulk soil, particles and colloids (Papers II and III)

The EXAFS measurements were performed on iron in the bulk soil, particles and colloids. The results from the shell fitting and wavelet transform analyses suggested that the iron in the bulk soil consisted of a mixture of ferrihydrite and monomeric iron, associated with soil organic matter, in all four soils, which is in agreement with Sjöstedt *et al.* (2013). The iron in soil particles also consisted of a mixture of ferrihydrite and monomeric iron associated with soil organic matter in Åsbro, Pukeberg and Vinterviken soil. The iron in the colloidal fraction most likely consisted of a mixture of ferrihydrite and iron associated with soil organic matter in Åsbro soil, whereas in Vinterviken and Gyttop soils the major phase was monomeric iron bound to soil organic matter. Using shell fitting, it was not possible to add a Fe-C distance in some of the samples. However, the wavelet transform plots visually indicated the presence of Fe-C interaction in all samples (Figure 14). According to Karlsson and Persson (2010), up to 25 % of hydrolysed iron might be present without showing up in wavelet transform plots.

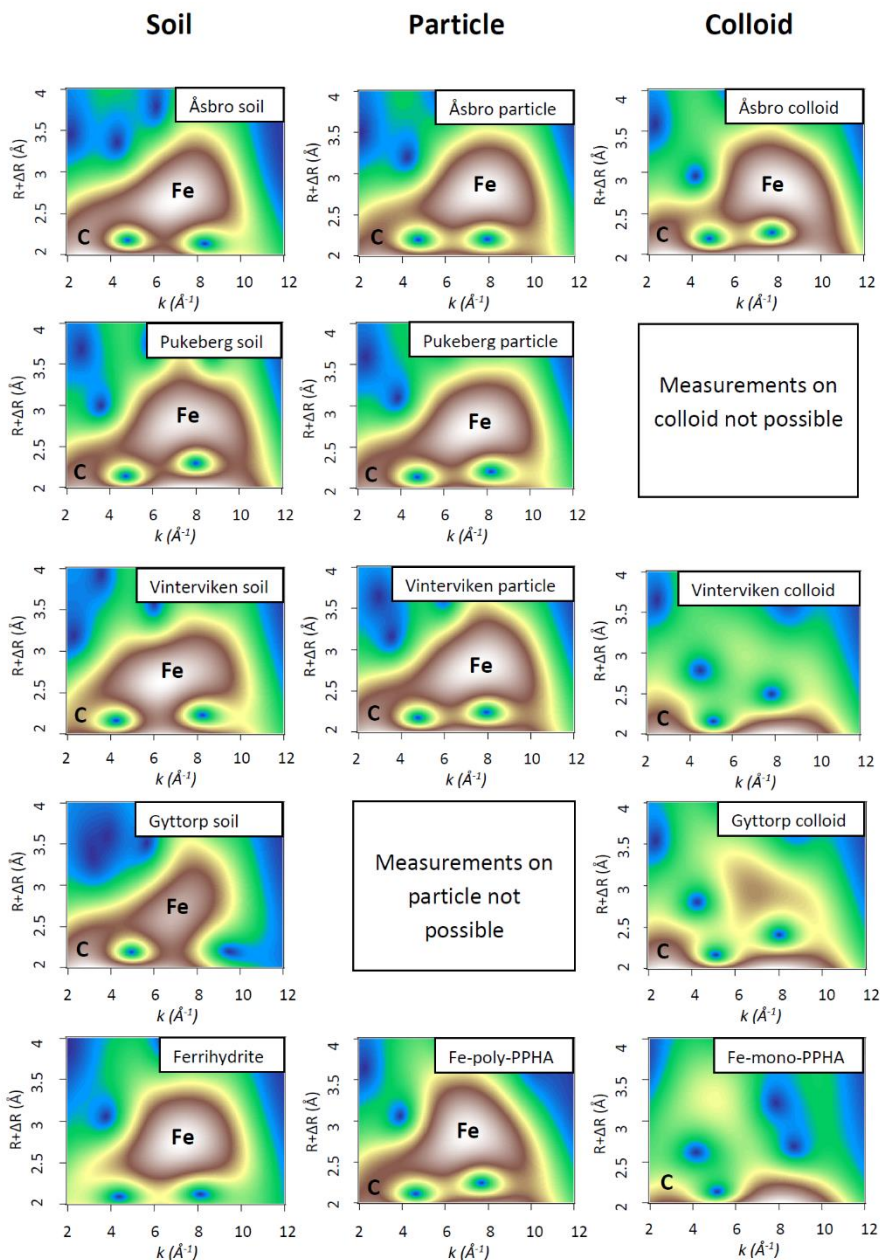


Figure 14. Wavelet transform graphs for iron (Fe) in samples and standards. The three bottom spectra are standards consisting of ferrihydrite (Kleja *et al.*, 2012), Fe-polymer-PPHA pH 6.9, Fe 88.1  $\mu\text{mol}$ , 100 mg PPHA (Karlsson & Persson, 2010) and Fe-monomer-PPHA, pH 3, Fe 8.97  $\mu\text{mol}$ , 100 mg PPHA (Karlsson & Persson, 2010). Due to too little material or too low concentrations, measurements could not be performed on some samples. The 'Fe' and 'C' in the graphs indicate where the Fe $\cdots$ Fe and Fe $\cdots$ C interaction is visible.

## 8.2 Partitioning of lead, chromium, zinc, arsenic and antimony (Paper II-IV)

This chapter presents the results on the partitioning of lead, chromium, zinc, arsenic and antimony between different size fractions in leachate obtained in the irrigation experiment using a rainfall intensity of  $2 \text{ mm h}^{-1}$  (Papers II-IV). In Paper II, a detailed speciation analysis of lead in particles and colloids was performed on all four soils. In Paper III, a detailed speciation analysis of chromium in particles and colloids was made for the Åsbro soil. Below, previously unpublished data on chromium leaching in the Vinterviken soil is also included.

In the Åsbro soil, most of the lead leached was found in the particle and colloid fractions. In the Pukeberg and Vinterviken soils, about 50 % of the total concentration of leached lead was found in these fractions, whereas in Gyttrorp soil the proportion was around 30 %. This high particulate and colloidal transport of lead is in agreement with previous findings (Denaix *et al.*, 2001; Pokrovsky *et al.*, 2005; Hu *et al.*, 2008; Pédrot *et al.*, 2008; Wang *et al.*, 2010; Yin *et al.*, 2010). The leaching pattern of lead is similar to that of iron and aluminium, suggesting that hydroxides of these elements might be important for the partitioning of lead.

In the Åsbro and Vinterviken soils, particulate and colloidal transport of chromium made up about 80 and 40 %, respectively (Figure 15). Interestingly, these were the two soils with the highest particulate and colloidal organic carbon leaching (Figure 13). In the Pukeberg and Gyttrorp soils, the total concentrations of chromium were below the detection limit. Large variation in particulate and colloidal transport of chromium has been seen in previous studies (Gasser *et al.*, 1994; Pédrot *et al.*, 2008; Wang *et al.*, 2010).

In the Åsbro soil, around 60 % of the total concentration of zinc was leached with particles and colloids, whereas in the Pukeberg, Vinterviken and Gyttrorp soils the proportion was <15 %. This variation in the tendency for zinc to be transported with particles and colloids confirms previous findings (Denaix *et al.*, 2001; Pokrovsky *et al.*, 2005; Pédrot *et al.*, 2008; Wang *et al.*, 2010). Zinc has a lower affinity for soil organic matter and hydroxides than lead (Lofts & Tipping, 1998), which might explain the lower tendency for zinc to be transported with particles and colloids.

Particulate and colloidal leaching of arsenic was <20 % and of antimony <5 %. Both arsenic and antimony have previously been indicated to have a low tendency for particle and colloidal transport (Pokrovsky *et al.*, 2005; Klitzke & Lang, 2009; Klitzke *et al.*, 2012).

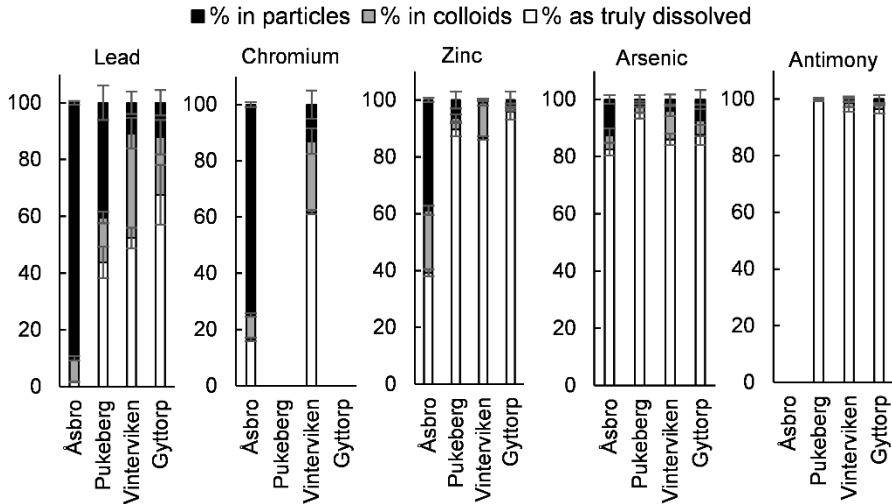


Figure 15. Particle (0.45 to 50  $\mu\text{m}$ ), colloid (10 kDa to 0.45  $\mu\text{m}$ ) and truly dissolved (<10 kDa) leaching of lead, chromium, zinc, arsenic and antimony from the four soils at irrigation intensity 2  $\text{mm h}^{-1}$ .

In general, the tendency for the metal(loid)s to be transported with particles and colloids followed the order: lead > chromium > zinc > arsenic > antimony. Particle and colloidal leaching of contaminants varied with the potential for adsorption to a specific sorbent; lead followed the same leaching pattern as iron, while chromium followed the same leaching pattern as organic carbon. This suggests that both the characteristics of the soil and the characteristics of the element govern the potential for these elements to be transported with particles and/or colloids.

### 8.2.1 Speciation of lead in particles and colloids (Paper II)

Published information on lead speciation in particles and colloids is scarce. However, a few quantitative studies have been performed on the potential carriers of lead in the particle and colloidal fractions in soil. These studies suggest that iron-rich compounds, possibly containing soil organic matter, transport lead in soils (Pokrovsky *et al.*, 2006; Pédrot *et al.*, 2008; Klitzke *et al.*, 2012). These results have been confirmed by qualitative measurements confirming the interaction between lead, iron and soil organic matter (Perdrial *et al.*, 2010; Neubauer *et al.*, 2013). However, little is known about the molecular speciation of lead in particles and colloids.

In this thesis work, lead speciation using EXAFS was performed on particles leached from Pukeberg and Vinterviken soils, and colloids leached from Vinterviken and Gyttorp soils. The EXAFS spectra suggested that the speciation of lead leached with particles and colloids was different from that in the solid soil (Figure 16). Hence, it was also possible to exclude the possibility that lead was mainly bound to soil organic matter. The presence of mineral phases of lead was excluded, based on the shape of the EXAFS spectra, the Pb-O distances and geochemical modelling (Figure 4, Table 3 and Table S7, all in Paper II). The larger or similar amplitude of the second peak ( $5.7 \text{ \AA}^{-1}$ ) compared with the first peak ( $3.7 \text{ \AA}^{-1}$ ) suggests a heavier back-scattering element (Figure 16), and the EXAFS spectra were similar to the Pb-ferrihydrate spectra. On the basis of the heavier second shell, a Pb-Fe distance was added to the model. In the particles, a Pb-Fe distance was obtained at  $\approx 3.32 \text{ \AA}$  (Table 3 in Paper II), which suggests an edge-sharing configuration (Scheinost *et al.*, 2001; Tiberg *et al.*, 2013). For the colloids, it was not possible to add a second shell because of background noise, but this does not exclude a potential contribution of a heavier back-scattering element, as indicated by the shape of the envelope of the EXAFS spectra.

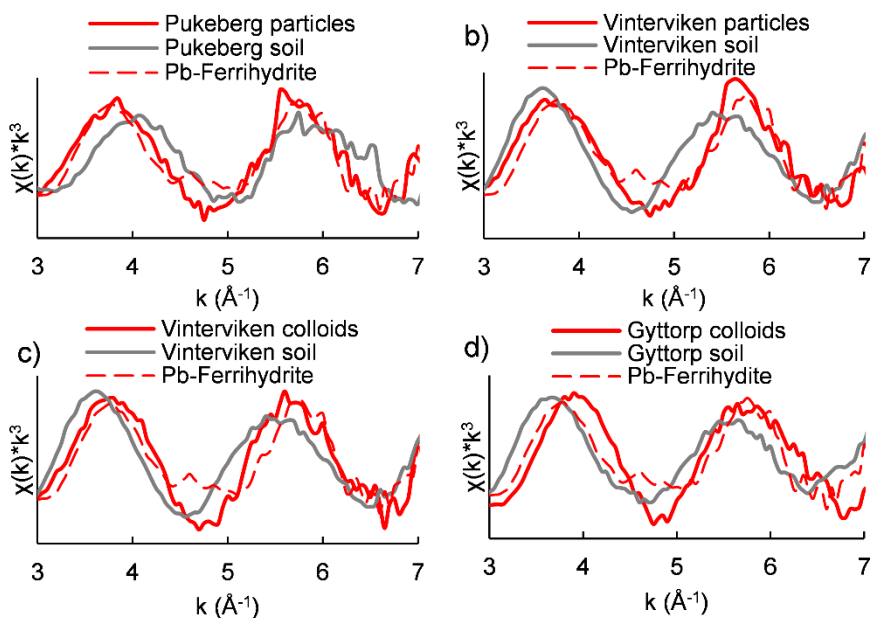
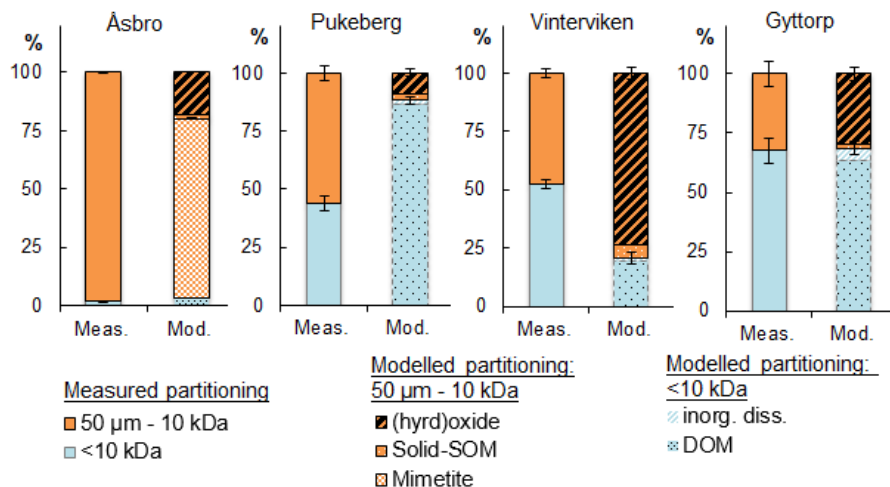


Figure 16.  $k^3$ -weighted extended X-ray absorption fine structure (EXAFS) spectra for lead in particles, colloids and bulk soil for all four soils, and in the Pb-Ferrihydrate standard (Tiberg *et al.*, 2013).

The results on the speciation of lead in particles and colloids, together with the iron EXAFS results, suggest that two end-members of lead species are present: Pb-ferrihydrate and Pb-soil organic matter. In the particles, iron was mainly found as ferrihydrate, and thus Pb-ferrihydrate can be assumed to be the major phase. In the colloids, monomeric iron bound to soil organic matter was identified as the major phase, but up to 25 % iron hydroxide might still be present (Karlsson & Persson, 2010). The EXAFS results for lead suggested complexation with ferrihydrate but, because of the abundance of soil organic matter, presence of both Pb-ferrihydrate and Pb-soil organic matter cannot be excluded.

Interestingly, it was also possible to describe the partitioning between the truly dissolved (<10 kDa) and the sum of ‘colloids plus particles’ (10 kDa to 50 µm) fractions using equilibrium geochemical modelling (*Figure 17*). The model set-up is described in detail in Paper II. The dominant lead species in the Pukeberg, Vinterviken and Gyttopp leachate was found to be lead bound to iron/aluminium hydroxides, in agreement with the EXAFS data. Moreover, adding mimetite as a possible solid phase in the model improved the description of the partitioning between truly dissolved and ‘colloids plus particles’ in the Åsbro soil leachate. The presence of mimetite was also indicated by the high arsenic concentrations interfering with lead EXAFS measurements on particles and colloids.



*Figure 17.* Measured partitioning and geochemically modelled partitioning and speciation of lead in ‘colloids plus particles’ (10 kDa to 50 µm) and truly dissolved (<10 kDa) fractions in the four soils.

## 8.2.2 Speciation of chromium in particles and colloids (Paper III)

As for lead, qualitative studies on potential carriers of chromium in particles and colloids are scarce. However, chromium has been found in correlation with iron, and it has been suggested that both iron and chromium are mobilised with soil organic matter (Gasser *et al.*, 1994; Pédrot *et al.*, 2008).

In this work, the speciation of chromium in the particles and colloids leached in the Åsbro soil was studied using EXAFS spectroscopy. Consistent with the speciation in the solid soil, chromium was identified as dimeric chromium(III)-SOM complexes (Figure 11, and Table 1 in Paper III). Using shell fitting, it was not possible to add a carbon contribution for these data. However, by performing wavelet transform plot analysis, it was possible to exclude the presence of heavier atoms, such as chromium in a chromium(III) tetrameric structure (Figure S6 in Paper III) (Gustafsson *et al.*, 2014). Hence, the dimeric chromium(III) complex bound to soil organic matter most likely dominated in the particles and colloids leached in the Åsbro soil.

The ability of a ‘generic model’ to describe the partitioning and speciation of chromium(III) in leachate from the Åsbro and Vinterviken soils was tested (unpublished data). The same ‘generic model’ set-up as for lead was used (Paper II), except that the Dzombak-Morel HFO (Hydrous Ferric Oxide) model (Dzombak & Morel, 1990) was used for sorption of chromium(III) to hydroxides, instead of the CD-MUSIC model (Hiemstra & van Riemsdijk, 2009; Tiberg *et al.*, 2013).

The model for the Åsbro soil overestimated the truly dissolved fraction of chromium to some extent, but the speciation obtained with the geochemical model showed dominance of dimeric chromium(III)-SOM complexes, which agreed with the EXAFS data (Figure 18). In the Vinterviken soil, the partitioning was described fairly well. According to the model, the speciation of chromium(III) in the ‘colloid plus particle’ fraction was mainly dimeric chromium(III)-SOM complexes (Figure 18).

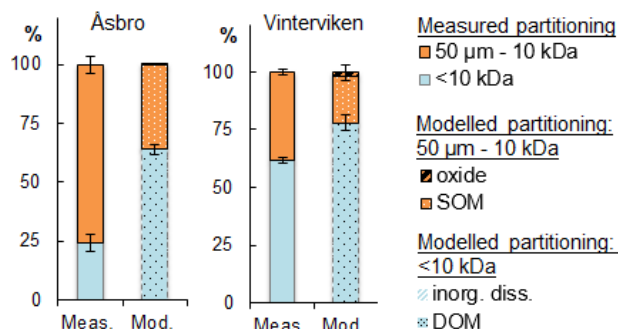


Figure 18. Measured partitioning and geochemically modelled partitioning and speciation of chromium in ‘colloids plus particles’ (10 kDa to 50 µm) and truly dissolved (<10 kDa) fractions in Åsbro and Vinterviken soils.

## 8.3 Effect of irrigation intensity on transport of lead and chromium

As discussed previously, the frequency of high-intensity rainfall events is expected to increase in some parts of Europe and North America as an effect of climate change (Pachauri & Meyer, 2014). Some studies indicate that this might result in increased leaching of particles and colloids (Lægdsmand *et al.*, 1999; Lægdsmand *et al.*, 2005; Yin *et al.*, 2010), although Jacobsen *et al.* (1997) suggest that higher rainfall intensities will have no effect on the leaching of particles and colloids. Furthermore, shorter contact time at higher irrigation intensities might affect the leaching of truly dissolved concentrations (Kim *et al.*, 2015).

An experiment performed as part of this thesis investigated the effect of irrigation intensity on the particulate, colloidal and truly dissolved concentrations of lead and chromium. Lead was selected for the analysis because of the extensive particulate and colloidal leaching of lead. For chromium, the focus was on the truly dissolved concentrations. Statistical analysis (ANOVA) was performed to examine the effect of irrigation intensity on the concentrations leached in each size fraction (0.45-50  $\mu\text{m}$ ; 10 kDa-0.45  $\mu\text{m}$ ; <10 kDa). The concentrations of lead and chromium in the leachate varied somewhat between replicate columns, so for visualisation purposes the concentrations in each size fraction were normalised to the concentration in the first sample (Figure 19 and Figure 20).

### 8.3.1 Effect of irrigation intensity on transport of lead (Paper II)

The results suggested that irrigation intensity affected the leaching of particulate, colloidal and truly dissolved lead differently, depending on soil (Figure 19 and Table 7). Increased irrigation intensity increased the leaching of particulate lead in the Pukeberg soil, but not in the in Vinterviken and Gyttop soils. The operational definition of particles was 0.45 to 50  $\mu\text{m}$ , which is a wide size range. The finer texture in the Vinterviken and Gyttop soils might have resulted in a smaller average size of particles mobilised compared with Pukeberg soil. Hence, the smaller particles in Vinterviken and Gyttop soil might be governed by leaching mechanisms more similar to those of colloids. Larger particles are more prone to be affected by increased shear stress (Kaplan *et al.*, 1993; Bergendahl & Grasso, 2003), while colloids are more affected by chemical perturbations (Bergendahl & Grasso, 2003). This resulted in no effect on the leaching of colloidal lead in Pukeberg soil, particulate and colloidal lead in Vinterviken soil or colloidal leaching in Gyttop soil. However, the decrease in particulate lead leached in Gyttop soil with increased irrigation intensity might be explained by

kinetically constrained particle release in that soil (Ryan & Gschwend, 1994; Jacobsen *et al.*, 1997; Bergendahl & Grasso, 2003).

In Åsbro soil, there was a decrease in particle and colloidal leaching with increasing irrigation intensity. However, it was not possible to evaluate whether this was an effect of irrigation intensity or depletion (Worrall *et al.*, 1993), since the last 2 mm h<sup>-1</sup> session is missing.

There was no decrease in truly dissolved lead concentrations at increasing irrigation intensities (Table 7), which is in agreement with the fast dissolution in the time-dependent batch solubility test (see Figure 8). Rather, an increase in the truly dissolved concentrations of lead was indicated in the Gyttop (shooting range) soil, which might be explained by increased contact between the water phase and residues of lead bullets (see Figure 6) at higher irrigation intensities.

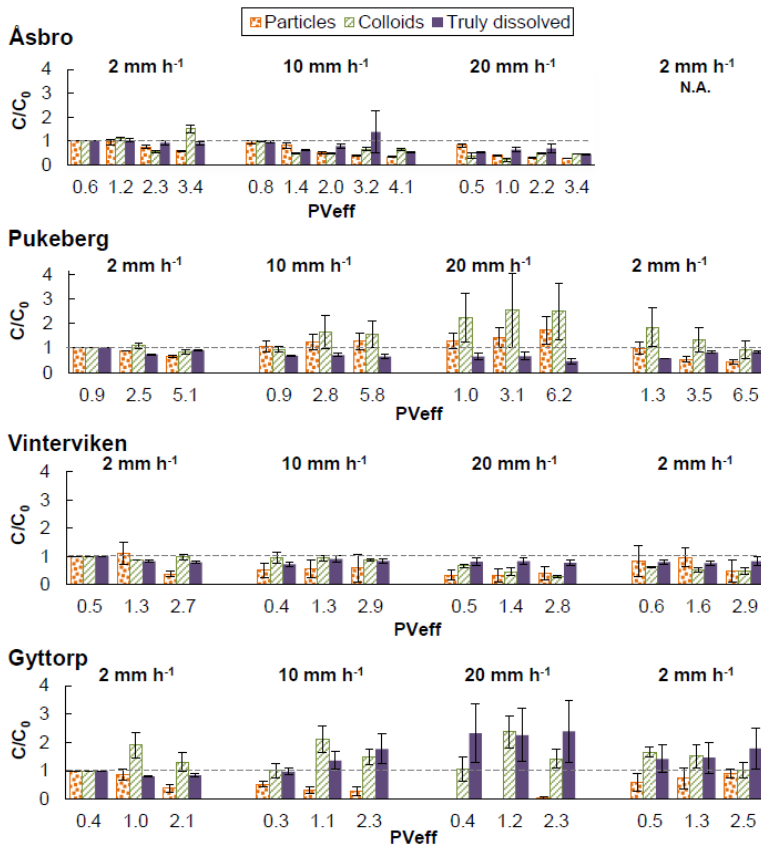


Figure 19. Effect of irrigation intensity on leaching of lead from the four soils. The concentration of the first sample ( $C_0$ ) was normalised to 1 and the following concentration ratios show concentration ( $C$ ) changes throughout the experiment. Error bars indicate standard error of the mean (SEM) for three (Gyttop, Pukeberg, Vinterviken) or four (Åsbro) soil columns.  $P_{Veff}$  = effective pore volume.

Table 7. Summary of statistical analyses on the effect of irrigation intensity on leaching of different lead (Pb) fractions from the four soils and suggested mechanisms responsible for the effect. Statistical data are presented in Supporting Information to Paper II. DOC = dissolved organic carbon. The \* indicated statistically significant effect of irrigation intensity.

Soil	Particle-bound Pb	Colloid-bound Pb	Truly dissolved Pb
Åsbro	Decrease, possibly because of depletion	Decrease, possibly because of depletion	Decrease, possibly because of decreased DOC leaching
Pukeberg	*Increase, because of increased shear	No significant change	No significant change
Vinterviken	No significant change	No significant change	No significant change
Gyttorp	*Decrease, possibly because of rate-limited diffusion processes	No significant change	*Increase, possibly because of increased leaching from residues of Pb bullets.

The effect of irrigation intensity on particle- and colloid-mediated transport of lead was small overall, at most a factor of three. Larger differences, up to one order of magnitude, in particle- and colloid-mediated transport of lead were observed between the soils. This suggests that soil properties have a greater influence on particulate and colloidal transport of lead than the irrigation intensity.

### 8.3.2 Effect of irrigation intensity on transport of chromium (Paper III)

In Paper III, the transport mechanisms of chromium in the Åsbro soil were studied thoroughly. In this section, unpublished data on chromium in the Pukeberg, Vinterviken and Gyttorp soils are also presented, in order to provide a more general picture of transport mechanisms for chromium in historically contaminated soils.

In the Åsbro soil, a decrease in the particulate fraction was observed with increasing irrigation intensity (Figure 20). However, for the Åsbro soil the last session of 2 mm h<sup>-1</sup> is missing and a potential effect of depletion (Worrall *et al.*, 1993) cannot be excluded. Interestingly, in the Vinterviken soil at a rainfall intensity of 20 mm h<sup>-1</sup>, the colloid-bound concentration of chromium was significantly lower than at the 2 and 10 mm h<sup>-1</sup> intensities (Figure 20). This suggests kinetically constrained colloidal release (Ryan & Gschwend, 1994; Jacobsen *et al.*, 1997; Bergendahl & Grasso, 2003). For colloidal lead in Vinterviken soil, a decrease in concentration with increasing irrigation intensity can be seen in Figure 19, but there was no significant effect of irrigation intensity on colloidal leaching of lead in that soil (Table 7). In Pukeberg and Gyttorp soil, the total concentrations of chromium were below the detection limit and hence the effect of irrigation intensity on leaching of particles and colloids could not

be determined. However, the method for measuring  $<0.45 \mu\text{m}$  and  $<10 \text{ kDa}$  fraction had a lower detection limit.

The concentration of chromium leached from the soils in the truly dissolved fraction is governed by equilibrium processes. In the Åsbro soil, the truly dissolved concentration of chromium was significantly higher in the  $2 \text{ mm h}^{-1}$  leachate than in the  $10$  and  $20 \text{ mm h}^{-1}$  leachates. This is consistent with the kinetically constrained dissolution indicated in the time dependent-solubility test (see Figure 8). In contrast, the leaching of truly dissolved chromium in Pukeberg, Vinterviken and Gyttop soil was not affected by the irrigation intensity (Figure 20), which is also in agreement with results from the time-dependent solubility batch test (Figure 8).

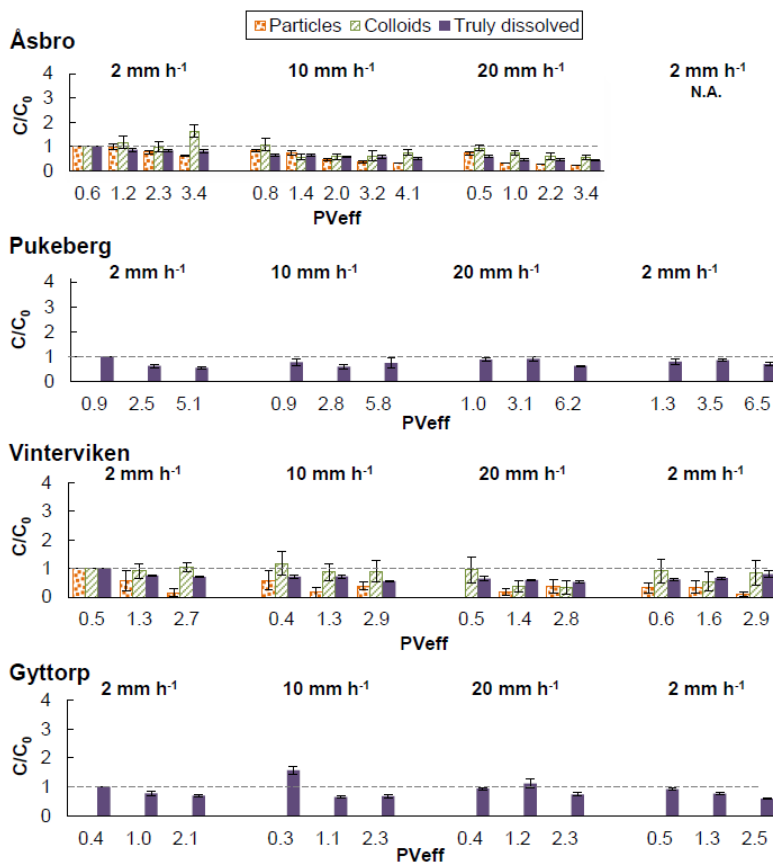


Figure 20. Effect of irrigation intensity on leaching of chromium from the four soils. The concentration of the first sample ( $C_0$ ) was normalised to 1 and the following concentration ratios show concentration ( $C$ ) changes throughout the experiment. Error bars indicate standard error of the mean (SEM) for three (Gyttop, Pukeberg, Vinterviken) or four (Åsbro) soil columns.  $P_{Veff}$  = effective pore volume.



## 9 Mechanisms controlling transport of lead and chromium in soils

### 9.1 Soil factors controlling leaching of particulate and colloidal lead (Paper II)

Because of the large differences in partitioning of lead between particles, colloids and truly dissolved fraction in the soils studied in this thesis, soil parameter(s) that may govern the partitioning of lead between ‘colloids plus particles’ (10 kDa to 50  $\mu\text{m}$ ) and truly dissolved (<10 kDa) fractions were investigated. Moreover, with the aim of reaching a more general understanding, a literature search was made for other studies using intact soils with a low clay content. With these two restrictions, only one study with two investigated soils qualified for the analysis (Yin *et al.*, 2010). The Åsbro soil was excluded from the analysis as the precipitation of mimetite might have caused the very high leaching of particulate and colloidal lead in this soil.

A number of soil factors, such as pH (Hu *et al.*, 2008), clay content (Vendelboe *et al.*, 2011; Norgaard, 2014), dexter  $n$  (clay/OC) (Norgaard, 2014), iron content (Seta & Karanthansis, 1996) and organic carbon content (Wang *et al.*, 2010), were investigated. However, these were all found to be poor predictors of ‘colloid plus particle’-bound leached lead ( $p=0.38-0.82$ ) for the soils used in this study. However, a weak relationship between sand content and ‘colloids plus particles’ was indicated by the analysis ( $R^2=0.46$ ,  $p=0.21$ ) (Figure 21). Furthermore, a functional relationship between sand content and the fraction of larger pores was indicated (Figure 21). A higher sand content results in larger pores and less straining (Vinten *et al.*, 1983), which might facilitate transport of particles and colloids. Hence, the sand content of a soil could possibly be used as a first indicator when identifying those non-macroporous soils with a high risk of particulate and colloidal leaching. However, this assumption might not

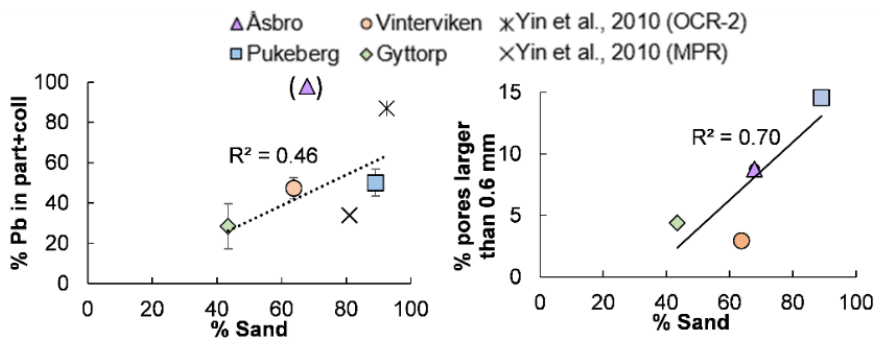


Figure 21. Soil properties governing ‘colloid plus particle’ (10 kDa to 50  $\mu\text{m}$ ) leaching of lead (Pb) in the four soils and in a previous study by Yin *et al.* (2010). The Åsbro soil was excluded from the analysis, see text for explanation.

be valid for macroporous soils (Seta & Karanthansis, 1996; Vendelboe *et al.*, 2011; Norgaard, 2014).

## 9.2 Conceptual model of lead and chromium leaching in non-macroporous soils

Based on the work presented in this thesis, a conceptual model of lead and chromium leaching in non-macroporous soils is presented in Figure 22. It was possible to describe the solubility of lead and chromium in the bulk soil, *i.e.* the partitioning between the solid phase and the truly dissolved phase, using geochemical equilibrium modelling. Moreover, it was possible to describe the partitioning of lead and chromium between truly dissolved and ‘colloid plus particle’ phases using chemical equilibrium calculations. This suggests that lead and chromium in all three compartments, *i.e.* ‘solid’, ‘truly dissolved’ and ‘colloid plus particle’ phases, were at or near equilibrium. Consequently, a feasible first approach to estimate the overall transport of lead and chromium in soils would be to use a simple  $K_d$  approach, where  $K_d$  is a conditional linear partitioning constant. Here,  $K_d$  is simply the total concentration of the elements in the solid phase divided by the total concentration in the mobile water phase, *i.e.* all species in the mobile water phase are added together into one concentration term. The  $K_d$  value is, of course, dependent on several factors, such as the concentrations of iron, aluminium and organic carbon in the ‘colloid plus particle’ phase, the truly dissolved concentration of organic carbon and the pH.

In a recent study, Babakhani *et al.* (2017) showed that the assumption of equilibrium between the solid phase and the solution phase of engineered nano-

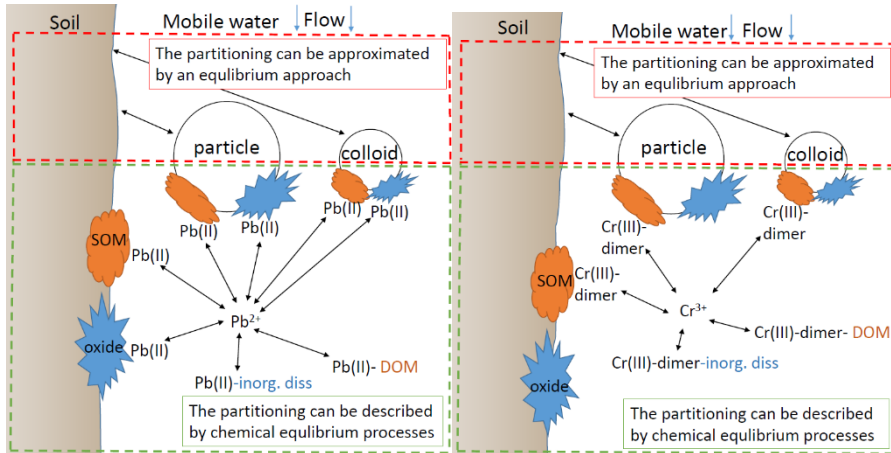


Figure 22. Conceptual model of the speciation and transport mechanisms of lead and chromium in contaminated soils. All arrows in the diagram indicate equilibrium.

particles in dynamic transport models gave better modelling results than more advanced kinetic terms in dynamic transport models. In the four soils investigated in this thesis, the dynamics of particle and colloidal transport in the irrigation experiment were quite rapid, as indicated by the fairly small effect of irrigation intensity on colloidal and particulate mobilisation of elements. Hence, it might be possible to use the  $K_d$  approach in a first step to describe the mobilisation of particles and colloids in non-macroporous soils (Figure 22).



## 10 Evaluation of three standardised leaching tests (Paper IV)

Irrigation experiments in combination with EXAFS speciation and geochemical modelling provided useful quantitative and qualitative information on the leaching mechanisms, especially of lead and chromium, in historically contaminated soils. However, these methods are advanced and time-consuming and would therefore not be feasible to perform in a standard risk assessment of contaminated sites. In 'normal' risk assessments, much simpler methods are used. The leachability of an element is usually described by a partitioning coefficient, the  $K_d$  value, defined as the ratio of the total concentration in the bulk soil to the concentration in solution at equilibrium (USEPA, 1999). The  $K_d$  value is usually estimated using either a batch test or percolation test using repacked soil columns. In the standard set-up, the leached solution is filtered through a 0.45  $\mu\text{m}$  filter and is considered the 'dissolved' fraction. With this approach, particle and colloidal leaching of metal(loid)s is normally not considered and the truly dissolved concentration might be estimated inaccurately (see Figure 1 and Figure 7). Furthermore, the experimental set-up can affect the outcome of the experiment. Differences in outcome when using a percolation test or a batch test or depending on the size fraction analysed have been reported (Chang *et al.*, 2001; Schuwirth & Hofmann, 2006). In addition, differences in liquid-to-solid ratio (L/S), leachant and contact time may all affect the concentrations leached (Chang *et al.*, 2001; Schuwirth & Hofmann, 2006; Centioli *et al.*, 2008; Fest *et al.*, 2008; Yasutaka *et al.*, 2017). Some studies have focused on evaluating standard leaching tests, by comparing the outcome from the leaching test to that obtained in realistic field-like conditions (MacDonald *et al.*, 2004; Schuwirth & Hofmann, 2006; Grathwohl & Susset, 2009), but the results are contradictory. Moreover, to the best of my knowledge, the ability of standard leaching tests to predict the leaching of particulate, colloidal and truly

dissolved fractions in realistic field-like conditions has not been examined previously.

To study how well the leaching tests commonly used in risk assessments describe the leaching of metal(loids), one percolation test and two batch tests were evaluated. The concentrations leached in the 2 mm h<sup>-1</sup> irrigation intensity were compared with the concentrations in the standardised leaching tests. To account for particulate, colloidal and truly dissolved leaching, the same size cut-off points as in the irrigation experiment were used for particles (0.45-8 µm, only percolation test), colloids (10 kDa-0.45 µm) and the truly dissolved fraction (<10 kDa). In the laboratory, a large soil column with an intact soil structure is as close to realistic field-like conditions as possible. It is possible to create a system where the hydrological conditions can be controlled and elements in the leachate can be size-fractionated shortly after sampling.

The samples used in the standardised leaching tests were taken from homogenised soil from the intact soil profiles used in the irrigation experiment. The experimental set-ups are summarised in Table 4 and the elements analysed in each soil are summarised in Table 8. Lead was chosen as a representative for cations with substantial particle- and colloid-facilitated leaching, while zinc was chosen because it is less likely to be leached with particles and colloids (Denaix *et al.*, 2001; Pédrot *et al.*, 2008). Arsenic was chosen as it is a redox-sensitive oxyanion, while antimony was chosen as an oxyanion that is reduced less efficiently compared to arsenic (Park *et al.*, 2018).

## 10.1 Evaluation of contact time

An essential aspect when evaluating different experimental set-ups is to assess whether the contact time between soil and leachant is long enough for the elements studied to reach a concentration (near) equilibrium.

The results of the time-dependent solubility test suggested that *e.g.* antimony in Pukeberg soil consisted of some phases with slower solubility (see Figure 8). However, the solubility of lead, zinc, arsenic and antimony in the other soils studied was shown to be fast, and near equilibrium conditions was reached within 24 hours.

Table 8. Elements evaluated for each contaminated site in standardised leaching tests

Site	Lead	Zinc	Arsenic	Antimony
Åsbro	x	x	x	
Pukeberg	x		x	x
Vinterviken	x	x	x	x
Gyttorp	x	x	x	x

In the irrigation experiment, the contact time varied between 31 and 80 hours in the 2 mm h<sup>-1</sup> irrigation intensity session for the different sites (Table S4 in Paper IV). In the standardised percolation test, the contact time ranged between 21 and 29 hours, depending on soil, while in the two batch tests the contact time was 24 hours (Table 4). Hence, based on findings in the time-dependent solubility batch test, it can be concluded that the truly dissolved concentration was at or near equilibrium in the irrigation experiment and in all three standardised leaching tests for most elements.

## 10.2 Percolation experiment (CEN/TS 14405)

In the percolation test, samples can be extracted at different liquid-to-solid ratios (L/S). The effect of liquid-to-solid ratio was most pronounced for the <8 µm fraction (Figure 23), especially for elements such as lead, iron and aluminium that are readily transported with particles and colloids (see Figure 15). However, on filtering the solution through a 0.45 µm filter or 10 kDa filter, the effect of liquid-to-solid ratio becomes less pronounced. Hence, it is mainly the particle fraction that is prone to artefacts arising from different liquid-to-solid ratios. The enhanced leaching of particles in the percolation test could be an effect of entrapped particles being made available when homogenising the soil (Massoudieh & Ginn, 2007; Yasutaka *et al.*, 2017) and the saturated conditions in the percolation test (Wan & Wilson 1994; Torkzaban *et al.*, 2008).

The concentrations of lead and zinc in the truly dissolved fraction were well predicted in the percolation test. In Papers I and II, lead was suggested to bind to organic carbon in the truly dissolved fraction and, since the organic carbon content was well predicted, the concentration of lead was similar in the irrigation experiment and the percolation test (Figure 23). The solubility of zinc is largely governed by pH (McBride *et al.*, 1997; Centioli *et al.*, 2008; Hernandez-Soriano *et al.*, 2013) but also by organic carbon (McBride *et al.*, 1997). The organic carbon concentration and the pH (Figure S6 in Paper IV) were both similar in the percolation test and the irrigation experiment, resulting in good prediction of truly dissolved zinc concentrations.

Even though arsenic was found to be mainly transported in truly dissolved form (Figure 15), the arsenic concentrations were overestimated in the percolation test (Figure 23 and Table 9). The truly dissolved manganese concentrations were also overestimated in the percolation test (Figure 23 and Table 9). Manganese is fairly easily reduced from MnO<sub>2</sub> to the soluble Mn<sup>2+</sup> (Borch *et al.*, 2010; Pan *et al.*, 2014), suggesting that reducing conditions occurred in the percolation test. Thus one possible explanation for the elevated

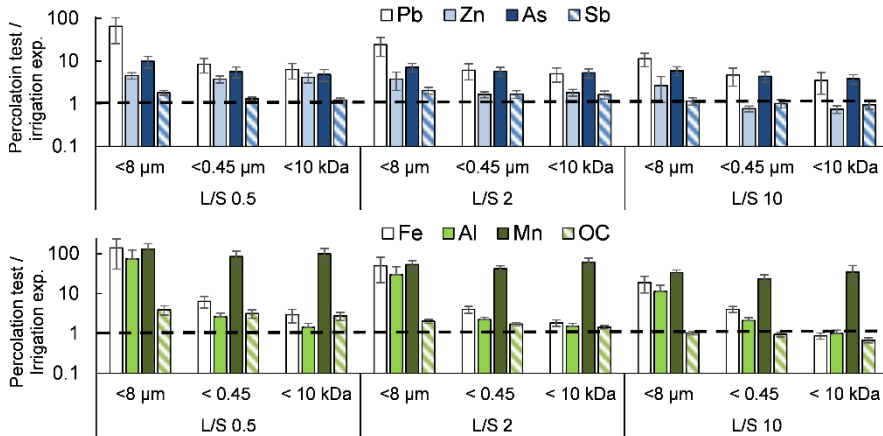


Figure 23. Mean ratio between concentrations of lead (Pb), zinc (Zn), arsenic (As), antimony (Sb), iron (Fe), aluminium (Al), manganese (Mn) and organic carbon (OC) measured in the percolation test and in the irrigation experiment for all four sites. The error bars indicate standard error of the mean (SEM). At a ratio of 1, the concentration in the percolation test is similar to that in the irrigation experiment.

Table 9. Mean ratio between concentrations of lead (Pb), zinc (Zn), arsenic (As) and antimony (Sb) measured in the standardised leaching test and the irrigation experiment. \*indicates that the log-transformed concentration obtained in the standardised leaching test was significantly different from the log-transformed concentration in the irrigation experiment ( $p < 0.05$ )

Element	Percolation test, L/S 10			H <sub>2</sub> O batch test		CaCl <sub>2</sub> batch test	
	<8 µm	<0.45 µm	<10 kDa	<0.45 µm	<10 kDa	<0.45 µm	<10 kDa
Pb	11.4*	4.7*	3.6	28.5*	5.5	25.3*	34.9
Zn	2.7	0.7*	0.7*	1.6	0.8*	3.0*	4.0*
As	6.3*	4.6*	3.8*	2.8*	3.8*	2.5	2.0
Sb	0.9	0.7	0.7	6.2	5.4	3.1	3.1

arsenic concentrations could be reduction of arsenic(V) to the more soluble arsenic(III) (Redman *et al.*, 2002; Borch *et al.*, 2010). However, antimony showed similar concentrations in the percolation experiment and in the irrigation experiment, possibly because of less efficient reduction of antimony(V) to antimony(III), compared to reduction of arsenic(V) to arsenic(III) (Mitsunobu *et al.*, 2006; Park *et al.*, 2018).

The percolation test has the potential to mimic leaching of particle and colloidal transport of lead. To test this potential, the percentage fractionation of lead into particles and colloids was determined in the percolation test at a liquid-to-solid ratio of 10 and in the irrigation test. The results suggest that particulate leaching of lead was overestimated in the percolation test for most soils and that the colloidal fraction was similar to the fractions obtained in the irrigation

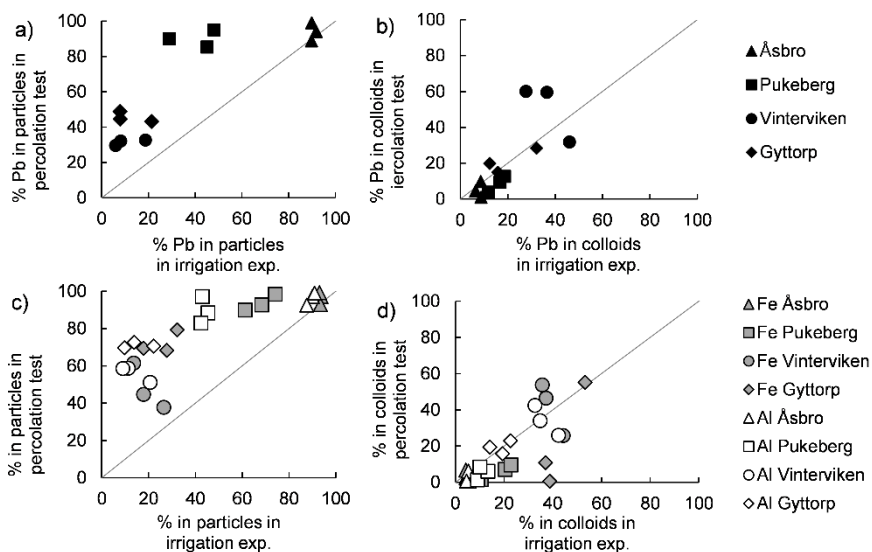


Figure 24. Ability of a percolation test at a liquid-to-solid ratio (L/S) of 10 to describe particulate and colloidal leaching of lead (Pb), iron (Fe) and aluminium (Al) from the four soils, compared with results from the irrigation experiment.

experiment. In addition, the leaching of iron and aluminium was similar to the leaching of lead. These results suggest that the percolation test can be used to obtain a conservative estimate of leaching of the particulate fraction for lead, iron and aluminium in risk assessments.

### 10.3 Batch test with deionised water (EN 12457-2)

In the H<sub>2</sub>O batch test, leaching of lead in the <0.45 μm fraction was overestimated, but for the <10 kDa fraction the concentrations were similar to those in the irrigation experiment (Table 9). A similar trend as for lead was seen for iron and aluminium (Figure 25). The enhanced colloidal mobilisation is most likely an effect of the lower ionic strength and homogenisation of the soil before the batch test (Massoudieh & Ginn, 2007; Torkzaban *et al.*, 2008; Yasutaka *et al.*, 2017). The truly dissolved concentrations of lead leached from Gyttorp were overestimated much more than those in the other three soils (dashed oval in Figure 25). This is most likely an effect of increased exposure of the residues of lead bullets (see Figure 6) after suspension of the soil in deionised water.

The leaching of arsenic was overestimated in the H<sub>2</sub>O batch test compared with the irrigation experiment (Table 9). In the batch test there is a head space of air, and the truly dissolved concentrations of manganese were similar to the concentrations in the irrigation experiment (Figure 25d), which suggests oxic

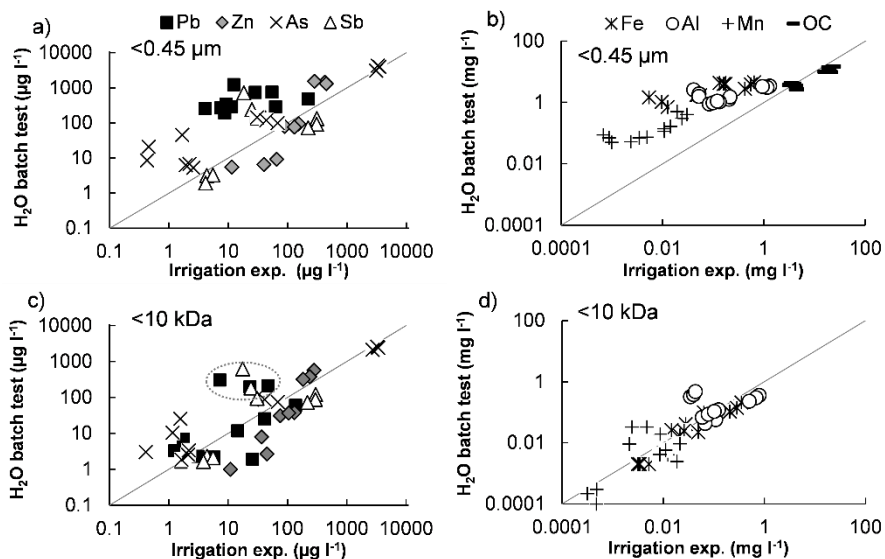


Figure 25. Ability of a  $H_2O$  batch test to describe leaching of lead (Pb), zinc (Zn), arsenic (As) and antimony (Sb), and iron (Fe), aluminium (Al), manganese (Mn) and organic carbon (OC), in different size fractions of the four soils. Data on dissolved organic carbon (DOC) concentrations in the truly dissolved fraction are not available. The grey dashed oval around the black squares in c) indicates the Gyttop soil.

conditions. Hence, the elevated concentrations of arsenic cannot not be explained by reducing conditions in the  $H_2O$  batch test. The concentrations of antimony in the  $H_2O$  batch test were similar to the concentrations obtained in the irrigation experiment.

The scattering of data for lead, zinc, arsenic and antimony in Figure 25 was larger than that for the indigenous elements iron, aluminium and manganese. This suggests a larger spatial variability of contaminating metal(loid)s, compared with the indigenous elements, in the intact soil columns. The indigenous elements can be expected to be more uniformly distributed because natural soil-forming processes govern their distribution in the soil.

#### 10.4 Batch test with 1 mM $CaCl_2$ (ISO/TS 21268-2)

In the  $CaCl_2$  batch test, the leaching of lead in the  $<0.45 \mu m$  fraction was similar to that in the irrigation experiment (Figure 26), although the ratio between the  $CaCl_2$  batch test and the irrigation experiment was fairly large. When the Gyttop soil was excluded the ratio was much smaller, 1.8 in the  $<0.45 \mu m$  fraction and 0.6 in the  $<10 kDa$  fraction. The addition of  $Ca^{2+}$  increases the ionic strength and compresses the electric double layer, which enhances the flocculation of colloids

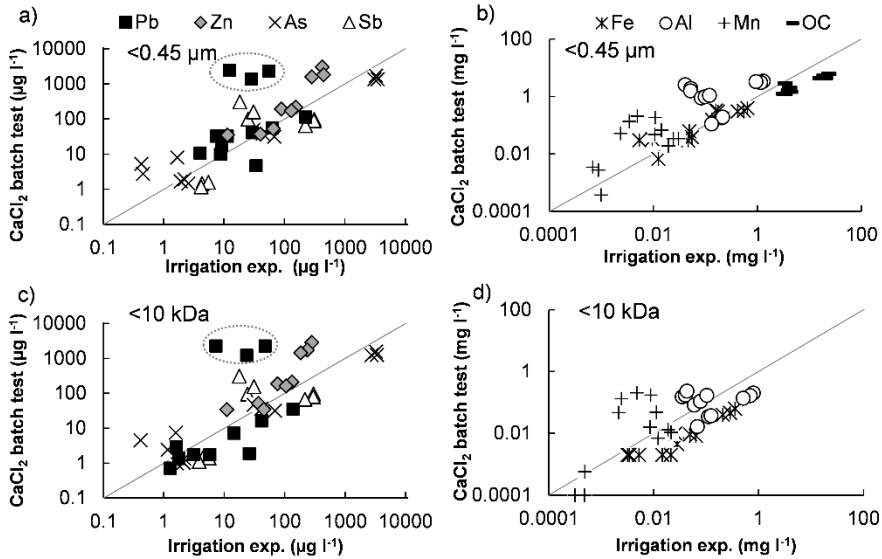


Figure 26. Ability of a  $\text{CaCl}_2$  batch test to describe leaching of lead (Pb), zinc (Zn), arsenic (As) and antimony (Sb), and iron (Fe), aluminium (Al), manganese (Mn) and organic carbon (OC), in different size fractions of the four soils. Data on dissolved organic carbon (DOC) concentrations in the truly dissolved fraction are not available. The grey dashed oval in a) and c) indicates the Gyttop soil.

and their attachment to the bulk soil (Kretzschmar & Sticher, 1997; Torzaban *et al.*, 2008). The larger overestimation for the Gyttop soil (dashed oval in Figure 26) compared with in the  $\text{H}_2\text{O}$  batch test might be explained by the lower pH (Fest *et al.*, 2008; Sjöstedt *et al.*, 2018).

The leaching of zinc was significantly overestimated in the  $\text{CaCl}_2$  test. This increase in solubility might be explained by cation exchange between calcium(II) and zinc(II), in combination with the lower pH (Figure S6 in Paper IV) (Voegelin *et al.*, 2003; Centioli *et al.*, 2008).

The  $\text{CaCl}_2$  batch test was the only standardised leaching test that could reflect the leaching of both arsenic and antimony. The lower pH in the  $\text{CaCl}_2$  batch test (Figure S6 in Paper IV) and addition of cations might lower the solubility of arsenic.

## 10.5 Which leaching test is preferred and why?

The choice of leaching test proved to be crucial for some elements studied in this thesis. Furthermore, the experimental set-up of the method chosen proved to be important for the interpretation of the results for some elements.

If particle leaching is suspected to be an important transport factor (*e.g.* for elements such as lead), the  $<8 \mu\text{m}$  fraction at a liquid-to-solid ratio (L/S) of 10 should be used for estimating the total transport. The amount of new available particles decreases with increasing liquid-to-solid ratio and thus the conditions in the repacked column in the percolation test became more similar to the intact soil columns in the irrigation experiment at higher liquid-to-solid ratio. The results also suggest that the percolation test can be used to categorise soils into high and low risk soils with respect to mobilisation of particulate and colloidal contaminants. Although the concentrations in the  $<8 \mu\text{m}$  fraction were overestimated at a liquid-to-solid ratio of 10 for most elements, the concentrations in the truly dissolved fraction were similar to those in the intact soils. However, care should be taken when applying the percolation test to redox-sensitive elements such as arsenic, as reducing conditions may occur in the saturated percolation test.

For arsenic, the  $\text{CaCl}_2$  batch test gave the most accurate results. If the standard set-up is used for a batch test ( $0.45 \mu\text{m}$ ), use of  $\text{CaCl}_2$  is preferable to  $\text{H}_2\text{O}$ , as the former gives a better estimate of the concentration of metal(loid)s in the truly dissolved fraction. Interestingly, antimony was well described using all three standardised leaching tests evaluated, although the lowest ratios were found in the percolation test.

Great heterogeneity in contaminant distribution in soil, *e.g.* as in the shooting range soil (Gyttorp), could result in too high concentrations being detected in the standardised leaching tests compared with intact soils (Figure 27). This might be explained by increased exposure of high concentration areas (*e.g.* lead bullets) in the batch test, whereas these were embedded in the soil matrix in the intact soils.

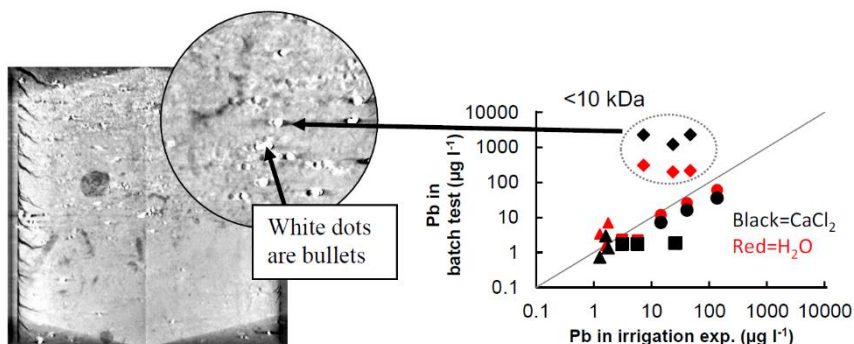


Figure 27. Example of a contaminated soil (Gyttorp, shooting range soil) with great heterogeneity in contaminant (lead, Pb) distribution and the effect on standardised batch test results.  $\Delta$ =Åsbro,  $\square$ =Pukeberg,  $\circ$ =Vinterviken,  $\diamond$ =Gyttorp.

## 11 Conclusions

- Particle- and colloid-mediated transport of lead(II) and chromium(III) from contaminated soils can be substantial. The partitioning between particulate, colloidal and truly dissolved forms in leachate is mainly governed by partitioning of iron for lead and by partitioning of organic carbon for chromium. Particle- and colloid-mediated leaching of zinc, arsenic and antimony is of less importance.
- Irrigation intensity has only a minor effect on leaching of particulate and colloidal lead and chromium from contaminated soils. This suggests that it is more important to consider soil properties, such as sand content, rather than investigating future scenarios of increased rainfall intensity when performing risk assessments.
- The speciation of lead in leached particles and colloids differs from that in the solid phase in contaminated soils. Thus, bulk soil speciation analysis is not a good indicator of the speciation of lead bound to particles and colloids that are eventually leached, except perhaps in situations where lead is precipitated as a mineral phase (as in the Åsbro soil).
- Dimeric chromium(III)-SOM complexes are suggested to govern the solubility in the bulk soil in all four contaminated soils studied and seem to be the major species in particles and colloids in Åsbro and Vinterviken soil.
- Geochemical equilibrium models with generic binding parameters can be used to describe the solubility and speciation of lead(II) and chromium(III) in the bulk soil, as well as the speciation in the leached particles and colloids, and the partitioning between 'colloids plus particles' and truly dissolved fractions.

- The truly dissolved concentration gives a well-defined fraction that can be used for calibration and/or validation of geochemical models describing the solubility of elements.
- The percolation test appears to overestimate the total leached concentration of certain elements such as lead, because of higher particulate mobilisation. However, using a liquid-to-solid ratio (L/S) of 10, instead of L/S 0.5 and 2, decreases the overestimation of particulate losses. Moreover, the percolation test at L/S 10 can be used to conservatively categorise soils into high- or low-risk soils with respect to mobilisation of particulate and colloidal contaminants.
- In a standard set-up of a batch test assessing the  $<0.45 \mu\text{m}$  fraction leached, 1 mM  $\text{CaCl}_2$  is preferred over deionised water as a leachant since the high  $\text{Ca}^{2+}$  concentration reduces colloidal mobilisation, avoiding overestimation of the concentration of elements such as lead. However, there is a risk of overestimating the concentration of weakly adsorbed elements, such as zinc, due to the higher  $\text{Ca}^{2+}$  concentration and a decrease in pH.

## 12 Environmental implications and future risk assessments

The properties of the soils studied in this thesis are probably common of those of contaminated soils in Sweden (see section 6.1). The low clay content in the four soils gave a low degree of preferential flow, which is in agreement with claims that macroporous flow only becomes important in soils with a clay content >9 % (Koestel *et al.*, 2012). Hence, absence of preferential flow is probably common in contaminated soils and a small effect of rainfall intensity could be expected in general for Swedish contaminated soils. However, in soils with a low degree of preferential flow, such as those studied here, particulate and colloidal transport may be substantial for certain elements such as lead and chromium. The results presented in this thesis suggest that sand content can be used as an indicator of the contribution of particulate and colloidal transport of lead to overall lead leaching, although more studies are needed to confirm and refine this relationship. However, this assumption should not be applied to macroporous, structured soils, as they have different factors governing the transport of particles and colloids, *e.g.* clay content (Vendelboe *et al.*, 2011; Norgaard, 2014).

Based on the results presented in this thesis, the speciation of lead and chromium in historically contaminated soils may be governed by soil properties and contaminant concentrations, and to a lesser extent by the speciation of the metal in the original contaminant entering the soil. Furthermore, the results suggest that equilibrium or near-equilibrium exists for lead and chromium between the major compartments in the soil system: the solid soil, particles, colloids and truly dissolved phase. One important practical implication of this finding is that generic geochemical models can be used for prediction of the speciation and solubility of metals in contaminated soils. These results are promising for increased future use of geochemical models in risk assessments, including predictions of free ion concentrations in ecotoxicity models and of

overall metal transport in the unsaturated and saturated zones using dynamic transport models.

A challenge when applying models is parameterisation and validation of the outcome of the model. In this thesis work, it was possible to validate the outcome of the model results on lead and chromium speciation with EXAFS data. However, this is seldom an option. Nonetheless, when using ‘generic model’ assumptions (Table 3), it was possible to describe the pH-dependent solubility of lead and chromium in a way that would be acceptable in most practical risk assessment situations. The model outcome using ‘generic model’ assumptions gave a good indication of the solubility control mechanisms. Furthermore, using geochemical modelling, it was possible to describe the solubility of lead also when the solubility was governed by a secondary mineral phase, such as for lead in the Åsbro soil. Hence, based on the results in this thesis, it is possible to recommend the use of a pH-dependent solubility test, preferably analysing the truly dissolved concentration (<10 kDa) of elements, in combination with geochemical modelling in site-specific risk assessments for lead and chromium.

## 12.1 Approach for future risk assessments

Based on the insights gained in this thesis, risk assessments should employ an approach that provides a deeper understanding of the mechanisms governing the transport and solubility of metal(loid)s. Here I suggest an approach to provide more accurate estimates on the transport of metal(loid)s in field situations using only standard methods. First, a step-by-step description should be made to determine a ‘transport  $K_d$ ’ value for non-macroporous soils (*i.e.* this method does not apply to soils with clay content  $\sim >10\%$ ). Second, a step-by-step method for speciation analysis for site-specific risk assessments should be performed.

### 12.1.1 ‘Transport $K_d$ ’ for non-macroporous soils

A method for determining a ‘transport  $K_d$ ’ value for non-macroporous soils is summarised in Figure 28. Step-by-step, the approach is as follows:

- 1 What is the clay content of the soil: a)  $<10\%$  or b)  $>10\%$ ?
  - a) Go to step 2.
  - b) This method cannot be applied to the particular soil.
- 2 What metal(loid) is being assessed: a) a metal with large tendency to be transported with particles and colloids, *e.g.* lead and chromium, or b) metal(loid)s with a low tendency to be transported with particles and colloids, *e.g.* zinc, arsenic and antimony?
  - a) Go to step 3.

- b) A batch test using 1 mM CaCl<sub>2</sub> as leachate and concentrations measured in the <0.45 μm fraction can be used to estimate the total leached concentration of metal(loid)s.
- 3 A metal with large tendency to be transported with particles and colloids is assessed. When not accounting for particulate and colloidal leaching, the total concentrations may be underestimated. However, as a conservative estimation, if the sand content is >50 %, particle and colloidal leaching may be substantial (see Figure 21). Does the soil have a sand content of: a) >50 % or b) <50 %?
- a) There are two feasible options to estimate the total leaching of metals, choose one:
- Perform a percolation test and analyse concentrations in both the <8 μm fraction and the <10 kDa fraction at L/S 10. This will give a conservative total concentration (<8 μm) leached and a well-defined truly dissolved concentration leached.
  - Perform a batch test using 1 mM CaCl<sub>2</sub> and filter the eluate through 0.45 μm. This concentration is fairly similar to the truly dissolved concentration. To account for the total concentration leached, add a safety factor, for example 10 for lead.
- b) A batch test using 1 mM CaCl<sub>2</sub> as leachate can be used to estimate the total concentration of leached metals.

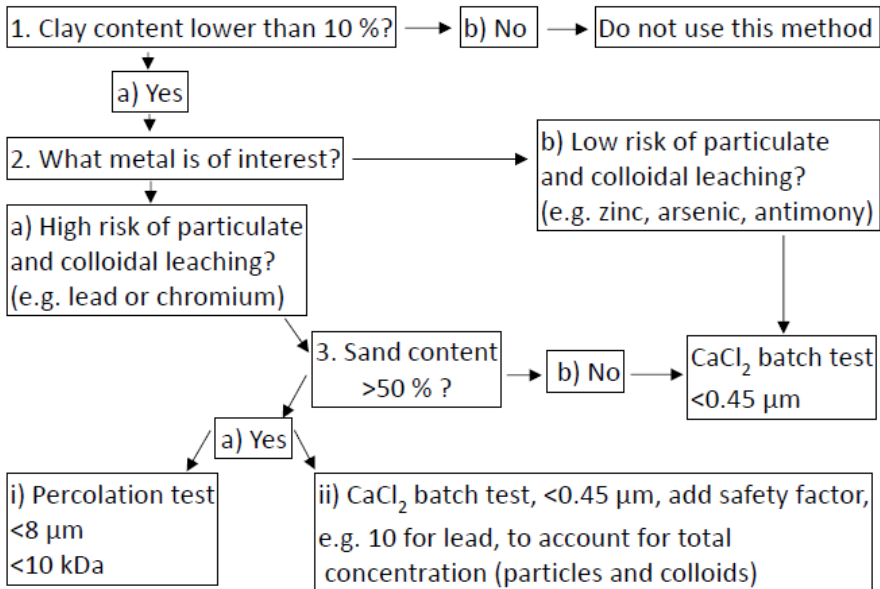


Figure 28. A suggested approach for obtaining a ‘transport K<sub>d</sub>’ value that accounts for both truly dissolved and total concentrations leached.

## 12.1.2 Geochemical modelling in risk assessments

A method for speciation analysis for site-specific risk assessment is summarised in Figure 29. Step-by-step, the approach is as follows:

- 1 Perform a pH-dependent solubility test, preferably over at least five pH values. Equilibrate the samples for 5 days. After equilibration, measure pH on unfiltered solution. Filter through a 10 kDa filter to obtain a well-defined truly dissolved fraction. Analyse cations, anions and DOC concentrations in the <10 kDa fraction. While the samples are equilibrating, measure geochemically active concentrations and oxalate-extracted concentrations of metals, as well as TOC in the bulk soil.
- 2 Use the extracted concentrations and TOC as input, and apply 'generic model' assumptions (Table 3) as described in Papers I and III, in the modelling tool, *e.g.* Visual MINTEQ. Allow the model to calculate the chemical equilibrium concentrations of truly dissolved metals at each pH value measured in the pH-dependent solubility test, assuming no precipitation of mineral phases. Compare the calculated truly dissolved concentrations with the measured truly dissolved concentrations from the pH-dependent solubility test.
  - i) The solubility is well described, and most likely also the speciation.
  - ii) The solubility is much overestimated in the model outcome. The solubility of the metals is probably not governed by adsorption, but by dissolution of a mineral phase. Hence, the  $K_d$  approach should not be used.

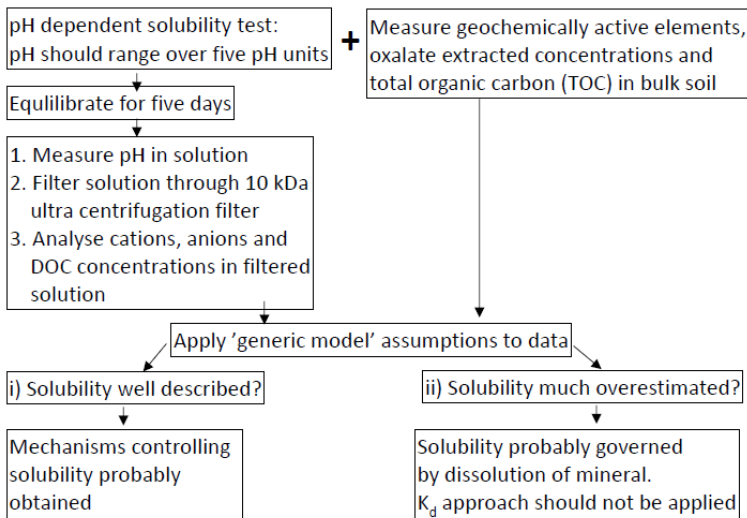


Figure 29. Simplified speciation analysis for site-specific risk assessments using the 'generic model' set-up.

## References

- Allaire, S. E., Roulier, S., Cessna, A. J. (2009). Quantifying preferential flow in soils: A review of different techniques. *Journal of Hydrology*. 378, 179–204.
- Babakhani, P., Bridge, J., Doong, R., Phenrat, T. (2017). Continuum-based models and concepts for the transport of nanoparticles in saturated porous media: A state-of-the-science review. *Adv Colloid Interface Sci*. 246, 75-104.
- Bajda, T. (2010). Solubility of mimetite  $Pb_5(AsO_4)_3Cl$  at 5-55°C. *Environ. Chem*. 7, 268-278.
- Bajnóczi, E.G., Pálinkó, I., Körtvéleysi, T., Bálint, S., Bakó, I., Sipos, P., Persson, I. (2014). Speciation and structure of lead(II) in hyper-alkaline aqueous solution. *Dalton Trans*. 43, 17539-17543.
- Ball, J. W. and Nordstrom, D. K. (1998). Critical evaluation and selection of standard state thermodynamic properties for chromium metal and its aqueous ions, hydrolysis species, oxides, and hydroxides. *J. Chem. Eng. Data*. 43, 895-918.
- Bergendahl, J. A. and Grasso, D. (2003). Mechanistic basis for particle detachment from granular media. *Environ. Sci. Technol*. 37, 2317-2322.
- Borch, T., Kretzschmar, R., Kappler, A., van Cappellen, P., Ginder-Vogel, M., Voegelin, A., Campbell, K. (2010). Biogeochemical redox processes and their impact on contaminant dynamics. *Environ. Sci. Technol*. 44, 15-23.
- Centioli, D., Comans, R. N. J., Gaudino, S., Galas, C., Belli. (2008). Leaching test: useful tool for the risk assessment of contaminates sediments. *Ann. Ist. Super. Sanità*. 44, 252-257.
- Chang, E. E., Chiang, P. C., Lu, P. H., Ko, Y. W. (2001). Comparisons of metal leachability for various wastes by extraction and leaching tests. *Chemosphere*. 45, 91-99.
- Crimp S. J., Spiccia, L., Krose, H. R., Swedde, T. W. (1994). Early stages of hydrolysis of chromium(III) in aqueous solution. 9. Kinetics of water exchange in the hydrolytic dimer. *Inorg. Chem*. 33, 465-470.
- Delsch, E., Basile-Delch, I., Rose, J., Masion, A., Borschneck, D., Hazemann, J-L., Macary, H, S., Bottero, J-Y. (2006). New combination of EXAFS spectroscopy and density fractionation for the speciation of Chromium within an andosol. *Environ. Sci. Technol*. 40, 7602-7608.
- Denaix, L., Semali, R. M., Duay, F. (2001). Dissolved and colloidal transport of Cd, Pb, and Zn in a silt loam soil affected by atmospheric industrial deposition. *Environ. Pollut*. 113, 29-38.

- Dijkstra, J. J., Meeussen, J. C. L., Comans, R. N. J. (2004). Leaching of heavy metals from contaminated soils: An experimental and modeling study. *Environ. Sci. Technol.* 38, 4390-4395.
- Ding, W., Stewart, D. I., Humphreys, P. N., Rout, S. P., Burke, I. T. (2016). Role of an organic carbon-rich soil and Fe(III) reduction in reducing the toxicity and environmental mobility of chromium(VI) at a COPR disposal site. *Sci. Total Environ.* 541, 1191–1199.
- Dzombak, D. A. and Morel, F. M. M. (1990). Surface complexation modelling: hydrous ferric oxide. Wiley-Interscience: New York, U.S.A.
- Elert, M., Fanger, G., Höglund, L.O., Jones, C., Suér, P., Wadstein, E., Bjerre-Hansen, J., Groen, C. (2006). Lakteter för riskbedömning av förorenade områden. *Naturvårdsverket, Swedish EPA*. Report 5535, pp 84. Stockholm, Sweden.
- Elzinga, E. J. and Cirno, A. (2010). Application of sequential extractions and X-ray absorption spectroscopy to determine the speciation of chromium in Northern New Jersey marsh soils developed in chromite ore processing residue (COPR). *J. Hazard. Mater.* 183, 145–154.
- Fest, P. M. J. E., Temminghoff, E. J. M., Comans, R. N. J., van Riemsdijk, W. H. (2008). Partitioning of organic matter and heavy metals in a sandy soil: Effects of extracting solution, solid to liquid ratio and pH. *Geoderma*, 146, 66-74. .
- Filella, M., Belzile, B., Chen, Y-W. (2002). Antimony in the environment: A review focused on natural waters II. Relevant solution chemistry. *Earth-Sci. Rev.* 59, 265-285.
- Filella, M. (2011). Antimony interactions with heterogeneous complexants in waters, sediments and soils: A review of data obtained in bulk samples. *Earth-Sci. Rev.* 107, 325-341.
- Funke, H., Scheinost, A.C., Chukalina, M. (2005). Wavelet analysis of extended x-ray absorption fine structure data. *Physic. Rev. B.* 71, 094110.
- Gasser, U. B., Juchler, S. J., Sticher, H. (1994). Chemistry and speciation of soil water from serpentinitic soils: importance of colloids in the transport of Cr, Fe and Ni. *Soil Sci.* 158, 314-322.
- Gee, G.W. and Bauder, J. W. (1986) Particle-size analysis. In *Methods of Soil Analysis, Part 1*, 2nd ed; Klute, A., SSSA, Inc., Madison, Wisconsin, USA, pp. 383-411.
- Grathwohl, P. and Susset, B. (2009). Comparison of percolation to batch and sequential leaching tests: Theory and data. *Waste Mang.* 29, 2681-2688.
- Guo, X., Wu, Z., He, M., Meng, X., Jin, X., Qiu, N., Zhang, J. (2014). Adsorption of antimony onto oxyhydroxides: adsorption behavior and surface structure. *J. Hazard- Mater.* 276, 339-345
- Gustafsson, J. P., Persson, I., Oromieh, A. G., van Schaik, J. W. J., Sjöstedt, C., Kleja, D. B. (2014). Chromium(III) complexation to natural organic matter: Mechanisms and modeling. *Environ. Sci. Technol.* 48, 1753-1761.
- Hashimoto, Y., Yamaguchi, N., Takaoka, M., Shiota, K. (2011). EXAFS speciation and phytoavailability of Pb in a contaminated soil amended with compost and gypsum. *Sci. Tot. Environ.* 409, 1001-1007.
- Hendrickx, J.M.H. and Flury, M., (2001). Uniform and preferential flow mechanisms in the vadose zone. In: *National Committee for Rock Mechanics (Eds.), Conceptual Models of Flow and Transport in the Fractured Vadose Zone*. National Academic Press, Washington, DC, USA. 149–187.

- Hernandez-Soriano, M. C., Peña, A., Mingorance, M. D. (2013). Soluble metals pool as affected by soil additions with organic inputs. *Environ. Toxicol. Chem.* 32, 1027-1032.
- Hiemstra, T. and van Riemsdijk, W. H. (2009). A surface structural model for ferrihydrite I: sites related to primary charge, molar mass, and mass density. *Geochim. Cosmochim. Ac.* 73, 4437-4451.
- Hopp, L., Nico, P. S., Marcus, M. A., Peiffer, S. (2008). Arsenic and chromium partitioning in a podzolic soil contaminated by chromated copper arsenate. *Environ. Sci. Technol.* 42, 6481-6486.
- Hu, S., Chen, X, Shi, J., Chen, Y., Lin. (2008). Particle facilitated lead and arsenic transport in abandoned mine sites soil influenced by simulated acid rain. *Chemosphere.* 71, 2091-2097.
- Inegbemor A. J., Thomas H., Williams P. A. (1989). The chemical stability of mimetite and distribution coefficients for pyromorphite mimetite solid-solutions. *Mineral. Mag.* 53, 363-371.
- Jacobsen, O. H., Moldrup, P., Larsen, C., Konnerup, L., Petersen, L. W. (1997). Particle transport in macropores of undisturbed soil columns. *J. Hydrol.* 196, 185–203.
- Jardine, P. M., Fendorf, S. E., Mayes, M. A., Larsen, I. L., Brooks, S. C., Bailey, B. (1999). Fate and transport of hexavalent chromium in undisturbed heterogeneous soil. *Environ. Sci. Technol.* 33, 2939-2944.
- Kaplan, D. I., Bertsch, P. M., Adriano, D. C., Miller, W. P. (1993). Soil-Borne mobile colloids as influenced by water flow and organic carbon. *Environ. Sci. Technol.* 27, 1193-1200.
- Karlsson, T. and Persson, P. (2010). Coordination chemistry and hydrolysis of Fe(III) in a peat humic acid studied by X-ray absorption spectroscopy. *Geochim. Cosmochim. Acta.* 74, 30–40.
- Kelly, S. D., Hesterberg, D., Ravel, B. (2008). Analysis of soils and minerals using X-ray absorption spectroscopy. In: Ulery, A. L. and Drees, L. R., (eds) *Methods of soils analysis. Part 5. Mineralogical methods.* SSSA Book Series, SSSA, Madison, WI, USA. pp. 387–464.
- Kim, J. and Hyun, S. (2015). Nonequilibrium leaching behavior of metallic elements (Cu, Zn, As, Cd, and Pb) from soils collected from long-term abandoned mine sites. *Chemosphere.* 134, 150-158.
- Kleja, D. B., van Schaik, J. W. J., Persson, I., Gustafsson, J. P. (2012). Characterization of iron in floating surface films of some natural waters using EXAFS. *Chem. Geol.* 326-327, 19-26.
- Klitzke, S., Lang, F., Kaipenjohann, M. (2008). Increasing pH releases colloidal lead in a highly contaminated forest soil. *Eur. J. Soil. Sci.* 59, 265-273.
- Klitzke, S. and Lang, F. (2009). Mobilization of soluble and dispersible lead, arsenic, and antimony in a polluted organic-rich soil – effects of pH increase and counterion valency. *J. Environ. Qual.* 38, 933-939.
- Klitzke, S., Lang, F., Kirby, J., Lombi, E., Hamon, R. (2012). Lead, antimony and arsenic in dissolved and colloidal fractions from an amended shooting-range soil as characterised by multi-stage tangential ultrafiltration and centrifugation. *Environ. Chem.* 9, 462–473.
- Klute, A. and Dirksen, C. (1986). Hydraulic conductivity and diffusivity: laboratory measurements. In: *Methods of soil analysis, Part 1, 2nd ed.* SSSA, Madison, Wisconsin, USA. pp. 687–734.

- Koestel, J. K., Moeys, J., Jarvis, N. J. (2011). Evaluation of nonparametric shape measures for solute breakthrough curves. *Vadose Zone J.* 10, 1261–1275.
- Kretzschmar, R. and Sticher, H. (1997). Transport of humic-coated iron oxide colloids in a sandy soil: influence of Ca<sup>2+</sup> and trace metals. *Environ. Sci. Technol.* 31, 3497-3504.
- Lægdsmand, M., Villholth, K. G., Ullum, M., Jensen, K. H. (1999). Processes of colloid mobilization and transport in macroporous soil monoliths. *Geoderma.* 93, 33–59.
- Lægdsmand, M., de Jonge, L. W., Moldup, P. (2005). Leaching of colloids and dissolved organic matter from columns packed with natural soil aggregates. *Soil Sci.* 170, 13-27.
- Landrot, G., Tappero, R., Webb, S. M., Sparks, D. L. (2012). Arsenic and chromium speciation in an urban contaminated soil. *Chemosphere.* 88, 1196–1201.
- Lin, Z., Comet, B., Qvarfort, U., Herbert, R. (1995). The chemical and mineralogical behavior of Pb in shooting range soils from central Sweden. *Environ. Pollut.* 89, 303-309.
- Liu, J., Aronsson, H., Ulén, B., Bergström, L. (2012). Potential phosphorus leaching from sandy topsoils with different fertilizer histories before and after application of pig slurry. *Soil Use Manage.* 28, 457-467.
- Lofts, S. and Tipping, E. (1998). An assemblage model for cation binding by natural particulate matter. *Geochim. Cosmochim. Acta.* 62, 2609-2625.
- MacDonald, J. D., Bélanger, N., Hendershot, W. H. (2004). Column leaching using dry soil to estimate solid-solution partitioning observed in zero-tension lysimeters. 2. Trace metals. *Soil and Sedim. Cont.* 13, 375-390.
- Manceau, A., Boisset, M.-C., Sarret, G., Hazemann, J.-L., Mench, M., Cambier, P., Prost, R. (1996). Direct determination of lead speciation in contaminated soils by EXAFS spectroscopy. *Environ. Sci. Technol.* 30, 1540-1552.
- Massoudieh, A. and Ginn, T. R. (2007). Modeling colloid-facilitated transport of multi-species contaminants in unsaturated porous media. *J. Contam. Hydrol.* 92, 162-183.
- McBride, M., Sauvé, S., Hendershot, W. (1997). Solubility control of Cu, Zn, Cd and Pb in contaminated soils. *Eur. J. Soil. Sci.* 48, 337-346.
- Minkina, T., Nevidomskaya, D., Bauer, T., Shuvaeva, V., Soldatov, A., Mandzhieva, S., Zubavichus, Y., Trigub, A. (2018). Determining the speciation of Zn in soils around the sediment ponds of chemical plants by XRD and XAFS spectroscopy and sequential extraction. *Sci. Total Environ.* 634, 1165-1173.
- Mitsunobu, S., Harada, T., Takahashi, Y. (2006). Comparison of antimony behavior with that of arsenic under various soil redox conditions. *Environ. Sci. Technol.* 40, 7270-7276.
- Neubauer, E., Schenkeveld, W. D. C., Plathe, K. L., Rentenberger, C., von der Kammer, F., Kraemer, S. M., Hofmann, T. (2013). The influence of pH on iron speciation in podzol extracts: Iron complexes with natural organic matter, and iron mineral nanoparticles. *Sci. Total Environ.* 461-462, 381-399.
- Norgaard, T. (2014). Linking soil bio-physical and structural properties to pesticide transport patterns across two loamy, agricultural fields. PhD Thesis, Science and Technology. Department of Agroecology, Aarhus University, Tjele.
- Pachauri, R. K. and Meyer, L. A. (2014). Climate Change 2014: Synthesis Report. Contribution of working groups i, ii and iii to the fifth assessment report of the Intergovernmental Panel on Climate Change. *IPCC*, Geneva, Switzerland.

- Pan, Y., Koopmans, G. F., Bonten, L. T. C., Song, J., Luo, Y., Temminghoff, E. J. M., Comans, R. N. J. (2014). Influence of pH on the redox chemistry of metal (hydr)oxides and organic matter in paddy soils. *J. Soils Sediments*. 14, 1713-1726.
- Park, J-H., Kim, S-J., Ahn, J., S., Lim, D-H., Han, Y-S. (2018). Mobility of multiple heavy metalloids in contaminated soil under various redox conditions: Effects of iron sulfide presence and phosphate competition. *Chemosphere*. 197, 344-352.
- Pédrot, M., Dia, A., Davranche, M., Bouhnik-Le Coz M., Henin O., Gruau G. (2008). Insights into colloid-mediated trace element release at the soil/water interface. *J. Colloid Interface Sci*. 325, 187-197.
- Perdrial, N., Perdrial, J. N., Delphin, J.-E., Elsass, F., Liewig, N. (2010). Temporal and spatial monitoring of mobile nanoparticles in a vineyard soil: evidence of nanoaggregate formation. *Eur. J. Soil Sci*. 61, 456-468.
- Persson, I., Lyczko, K., Lundberg, D., Eriksson, L., Placzek, A. (2011). Coordination chemistry study of hydrated and solvated lead(II) ions in solution and solid state. *Inorg. Chem*. 50, 1058–1072.
- Peterson, M. L., Brown Jr, G. E., Parks, G. A., Stein, C. L. (1997). Differential redox and sorption of Cr(III/VI) on natural silicate and oxide minerals: EXAFS and XANES results. *Geochim. Cosmochim. Acta*. 61, 3399-3412.
- Pilarski, J., Waller, P., Pickering, W. (1995). Sorption of antimony species by humic acid. *Water Air Soil Pollut*. 84, 51-59.
- Pokrovsky, O. S., Dupré, B., Schott, J. (2005). Fe-Al-organic colloids control of trace elements in peat soil solutions: results of ultrafiltration and dialysis. *Aquat. Geochem*. 11, 241-278.
- Pokrovsky, O. S., Schott, J., Dupre, B. (2006). Trace element fractionation and transport in boreal rivers and soil porewaters of permafrost-dominated basaltic terrain in Central Siberia. *Geochim. Cosmochim. Acta*. 70, 3239-3260.
- Ravel, B. and Newville, M. (2005). Athena Artemis Hephaestus: data analysis for X-ray absorption spectroscopy using IFEFFIT. *J. Synchrotron Rad*. 12, 537–541.
- Ravel, B. (2001). ATOMS: crystallography for the X-ray absorption spectroscopist. *J. Synchrotron Rad*. 8, 314–316.
- Redman, A. D., Macalady, D. L., Ahmann, D. (2002). Natural organic matter affects arsenic speciation and sorption onto hematite. *Environ. Sci. Technol*. 36, 2889-2896.
- Ryan, J. N. and Geschwend, P. M. (1994). Effects of ionic strength and flow rate on colloid release: Relating kinetics to intersurface potential energy. *J. Colloid. Interf. Sci*. 164, 21-34.
- Scheckel, K. G. and Ryan, J. A. (2004). Spectroscopic speciation and quantification of lead in phosphate-amended soils. *J. Environ. Qual*. 33, 1288–1295.
- Scheinost, A. C., Abend, S., Pandya, K., I., Sparks, D. L. (2001). Kinetic controls on Cu and Pb sorption by ferrihydrite. *Environ. Sci. Technol*. 35, 1090-1096.
- Scheinost, A. C., Rossberg, A., Ventlon, D., Xifra, I., Kretzschmar, R., Leuz, A-K., Funke, H., Johnson, C., A. (2006). Quantitative antimony speciation in shooting range soils by EXAFS spectroscopy. *Geochim. Cosmochim. Acta*. 70, 3299-3312.
- Schuwirth, N. and Hofmann, T. (2006). Comparability of and alternatives to leaching tests for the assessment of the emission of inorganic soil contamination. *J. Soils and Sediments*. 6, 102-112.

- Seta, A. K. and Karanthansis, A. D. (1996). Water disperseable colloids and factors influencing their dispersibility from soil aggregates. *Geoderma*. 74, 255-266.
- Sjöstedt, C., Persson, I., Hesterberg, D., Kleja, D. B., Borg, H., Gustafsson, J. P. (2013). Iron speciation in soft-water lakes and soils as determined by EXAFS spectroscopy and geochemical modelling. *Geochim. Cosmochim. Acta*. 105, 172-186.
- Slowey, A. J., Johnson, S. B., Newville, M., Brown Jr., G. E. (2007). Speciation and colloid transport of arsenic from mine tailings. *Appl. Geochem*. 22, 1884-1898.
- Spiccia, L. (1991). Early stages of the hydrolysis of chromium(III) in aqueous-solution - 7. Kinetics of cleavage of the hydrolytic dimer in acidic solution. *Polyhedron*. 10, 1865-1872.
- Stumm, W. (1992). Chemistry of the soil-water interface. *John Wiley & Sons*, New York, U.S.A.
- Swedish EPA. (2009). Riktvärden för förorenad mark. Modellbeskrivning och vägledning. *Swedish EPA, Report: 5976*. pp: 272. Stockholm, Sweden.
- Swedish EPA. (2018). Lägesbeskrivning av arbetet med efterbehandling av förorenade områden 2017. NV-02293-17. *Swedish EPA*. Dated: 2018-04-15. Stockholm, Sweden. pp. 48.
- Tella, M. and Pokrovski, G. S. (2012). Stability and structure of pentavalent antimony complexes with aqueous organic ligands. *Chem. Geol.* 292-293, 57-68.
- Tiberg C., Sjöstedt C., Persson I., Gustafsson J. P. (2013). Phosphate effects on copper(II) and lead(II) sorption to ferrihydrite. *Geochim. Cosmochim. Acta*. 120, 140-157.
- Tiberg, C., Kumpiene, J., Gustafsson, J. P., Marsz, A., Persson, I., Mench, M., Kleja, D. B. (2016). Immobilization of Cu and As in two contaminated soils with zero-valent iron – Long-term performance and mechanisms. *Appl. Geochem*. 67, 144-152.
- Tiberg, C., Sjöstedt, C., Gustafsson, J.P. (2018). Metal sorption to Spodosol Bs horizons: organic matter complexes predominate. *Chemosphere*. 196, 558-565.
- Tokunaga, T., Wan, J., Firestone, M. K., Hazen, T. C., Schwartz, E., Sutton, S. R., Newville, M. (2001). Chromium diffusion and reduction in soil aggregates. *Environ. Sci. Technol.* 35, 3169-3174.
- Torkzaban, S., Bradford, S. A., van Genuchten, M. T., Walker, S. L. (2008). Colloid transport in unsaturated porous media: The role of water content and ionic strength on particle straining. *J. Contam. Hydrol.* 96, 113-127.
- USEPA. (1999). Understanding variation in partition coefficient,  $K_d$ , values. Volume I: The  $K_d$  model, methods and measurements, and application of chemical reaction codes. *United States EPA*, office of air and radiation. Washington DC. Pp: 212.
- Vantelon, D., Lanzirotti, A., Scheihorst, A. C., Kretzschmar, R. (2005). Spatial distribution and speciation of lead around corroding bullets in a shooting range soil studied by micro-X-ray fluorescence and absorption spectroscopy. *Environ. Sci. Technol.* 39, 4808-4815.
- Vendelboe, A. L., Moldrup, P., Heckrath, G., Jin, Y., de Jonge, L. W. (2011). Colloid and phosphorus leaching from undisturbed soil cores sampled along a natural clay gradient. *Soil Sci.* 176, 399-406.
- Vinten, A. J. A., Yaron B., Nye, P. H. (1983). Vertical transport of pesticides into soil when adsorbed on suspended particles. *J. Agr. Food chem.* 31, 662-664.
- Voegelin, A., Barmettler, K., Kretzschmar, R. (2003). Heavy metal release from contaminated soils: Comparison of column leaching and batch extraction results. *J. Environ. Qual.* 32, 865-875.

- Vogel, T., Lichner, L., Dusek, J., Cipakova, A. (2007). Dual-continuum analysis of a cadmium tracer field experiment. *J. Contam. Hydrol.* 92, 50–65.
- Wan, J. and Wilson, J. L. (1994). Colloid transport in unsaturated porous media. *Water Resour. Res.* 30, 857-864.
- Wang, W., Wen, B., Zhang, S., Shan, X.-Q. (2010). Distribution of heavy metals in water and soil solutions based on colloid-size fractionation. *Intern. J. Environ. Anal. Chem.* 83, 357–365
- Wilkinson. K. and Lead, R. (2007). *Environmental Colloids and Particles: Behaviour, Separation and Characterisation*. Wiley, Hoboken, NJ, USA. Pp. 707, 1-15.
- Wilson, S. C., Lockwood, P. V., Ashley, P. M., Tighe, M. (2010). The chemistry and behaviour of antimony in the soil environment with comparisons to arsenic: A critical review. *Environ. Pollut.* 158, 1169-1181.
- Wittbrodt, P. R. and Palmer, C. D. (1996). Effect of temperature, ionic strength, background electrolytes, and Fe(III) on the reduction of hexavalent chromium by soil humic substances. *Environ. Sci. Technol.* 30, 2470-2477.
- Worrall, F., Parker, A., Rae, J. E, Johanson, A. C. (1993). Suspended and colloidal matter in the leachate from lysimeters: Implications for pesticide transport and lysimeter studies. *Brighton crop protection conference – weeds*. 899-904.
- Xu, C.-F.; Krouse, H. R.; Swaddle, T. W (1985). Conjugate base pathway for water exchange on aqueous chromium(III): variable-pressure and -temperature kinetic study. *Inorg. Chem.* 24, 267–270.
- Yasutaka, T., Imoto, Y., Kurosawa, A., Someya, M., Higashino, K., Kalbe, U., Sakanakura, H. (2017). Effects of colloidal particles on the results and reproducibility of batch leaching tests for heavy metal-contaminated soil. *Soils Found.* 57, 861-871.
- Yin X., Gao B., Saha U. K., Sun H., Wang G. (2010). Colloid-facilitated Pb transport in two shooting-range soils in Florida. *J. Haz. Mat.* 177, 620-625.
- Zhang, H. and Selim H. M. (2007). Colloid mobilization and arsenite transport in soil columns: effect of ionic strength. *J. Environ. Qual.* 36, 1273–1280.



## Acknowledgements

This PhD project was funded by the Swedish Research Council for Environment, Agricultural Sciences and Spatial Planning (FORMAS) (number 219-2012-868), to which I am very grateful. Part of the laboratory costs for paper IV was funded by J. Gust. Richert stiftelse (number 2015-00172), to which I am also very grateful.

Essential parts of this work were performed at synchrotrons, and I am truly grateful for the granted time slots and support from the beam line staff at beam line I811 at Max-lab in Sweden and beamline 4-1 and 11-2 at Stanford Synchrotron Radiation Lightsource (SSRL) in the USA.

A special thank you goes to my supervisory group for giving me the opportunity to work in this project. A big thank you to my main supervisor Dan Berggren Kleja, for sharing your knowledge on soil chemistry and always being willing to have scientific discussions, and for constantly being positive and encouraging throughout the years. Thank you Carin Sjöstedt for teaching me and supporting me in EXAFS data analysis and geochemical modelling. Thank you Ingmar Persson for teaching me the theory of EXAFS and EXAFS data collection (and always picking up the phone in the middle of the night when I was performing measurements at Max-lab). Thank you Jon Petter for rewarding discussions on EXAFS and geochemical modelling. Thank you Mats Larsbo for your soil physics evaluations and analyses, it was an essential part of this work. Thank you Geert for great input on the colloid transport discussions. Thank you Yvonne Andersson-Sköld for support and always being interested in the progress of the work.

Thank you to all the present and former members of kaffeklubben and the roomies I have had throughout the years! Thank you for the scientific discussions, but most of all for the non-scientific discussions.

Thank you Anna Mårtensson, Magnus Simonsson and Mats Larsbo for valuable comments on this thesis. A big thank you to my co-author Kristin Boye for performing EXAFS measurements at SSRL and for valuable comments on

Paper I and Paper II. Additionally, I want to thank Michael Petterson for help with field work, and Gunilla Theorin for help with laboratory work, as well as Claudia von Brömssen for help with the statistical analysis and Mary McAfee for language check of manuscripts and the thesis.

I am also very grateful to Sweco, where I have worked 20 % throughout this PhD project. Big thanks to my group, 1125, for always making me feel welcome when I randomly show up at the office. Special thanks to my manager Anna Brunsell, who has made it easy for me to combine two challenging jobs.

Last, but not least, a huge thank you to my family. To my husband, Peder, who always believes in me and for making outstanding lunchboxes. To my mum, dad, brother and sister for always being encouraging and for being the ones that you are.